Modelling Spatial Average Speeds in Switzerland during the COVID-19 Lockdown

Emanuel Zwyssig

Prof. Dr. Kay W. Axhausen (Supervisor)

Prof. Dr. Fadoua Balabdaoui (Supervisor)

Dr. Georgios Sarlas (Supervisor)

Thomas Schatzmann (Supervisor)

Semester Thesis **June 25 2021**

IVT Institut für Verkehrsplanung und Transportsysteme
Institute for Transport Planning and Systems

ETH
Eidgenössische Technische Hochschule Zürich
Swiss Federal Institute of Technology Zurich

Modelling Spatial Average Speeds in Switzerland during the COVID-19 Lockdown

Emanuel Zwyssig
D-MATH
ETH Zürich
CH-8093 Zurich
emzwyssi@ethz.ch

Prof. Dr. Kay W. Axhausen (Supervisor)
D-BAUG
ETH Zürich
CH-8093 Zurich

Prof. Dr. Fadoua Balabdaoui (Supervisor)
D-MATH
ETH Zürich
CH-8093 Zurich

Dr. Georgios Sarlas (Supervisor)
D-BAUG
ETH Zürich
CH-8093 Zurich

Thomas Schatzmann (Supervisor)
D-BAUG
ETH Zürich
CH-8093 Zurich

June 25 2021

Abstract

This semester thesis investigates how a large data set on mobility in Switzerland before and during the COVID-19 pandemic obtained by the Institute for Transport Planning and Systems at ETH via app-based GPS tracking can be used to model spatial average speeds. The data is described and possible issues relating to data quality are illustrated. After data cleaning, spatial average speeds are modelled for the whole country of Switzerland as well as smaller regions. Combining data from the pre-COVID-19 period as well as the COVID-19 lockdown was found to allow for modelling of the spatial average speed based on the number of distinct users observed in an area.

Keywords

COVID-19, Spatial Average Speeds

Contents

List of Tables

List of Figures

1 Introduction

1.1 The impact of COVID-19 on transport demand

During the first wave of the COVID-19 pandemic in spring of 2020, the Federal Council of Switzerland enacted a variety of non-pharmaceutical interventions to curb the spread of disease. For the duration of the lockdown starting March 16, restaurants, bars and stores selling non-essential items were closed. All public events were prohibited, and the population was asked to avoid unnecessary contacts and remain at home (Federal Council (2020)). After April 27, the measures were successively eased (Federal Office of Public Health FOPH (2020)).

The measures introduced had a noticeable impact on transport demand in Switzerland. While the effects were most pronounced for public transport, the call to limit social interactions and work from home also reduced the average daily distance travelled by car by up to 40%. This also lead to an increase in road speeds, especially during the morning and evening rush hours (Molloy *et al.* (2021)).

Similar changes in traffic demand and speed were observed in other European countries with comparable containment measures at the same time. In the city of Rome, the decrease in traffic lead to speed increases of up to 75% during the lockdown compared to the times before COVID-19 (Aletta *et al.* (2020)). On a stretch of national road in Czechia, a comparison of speeds of two days before and during the lockdown showed an increase in the average speed of up to 40% (Harantová *et al.* (2020)).

1.2 Modelling spatial average speed

The relationship between traffic volume and traffic speed is central to transport research, as it has many implications in transport policy and infrastructure appraisal. One approach is modelling this relationship on a link level. For this, a variety of different functional forms have been used in practice (see de Dios Ortúzar and Willumsen (2011) for an overview).

Another approach tries to find the relationship between traffic flow, density and speed for entire neighborhoods or cities, determining the macroscopic fundamental diagram (MFD). It has many desirable features, such as low demand for personal data and direct

applications in e.g. perimeter control. However, it requires areas of high traffic homogeneity to be estimated precisely. Futhermore, it ideally requires a combination of both floating car and loop dedector data. For an implementation of this approach, see Ambühl *et al.* (2017).

1.3 Aim of this paper

The Institute for Transport Planning and Systems (IVT) at ETH has recorded a large data set on mobility behavior both before and during the COVID-19 lockdown. The aim of this paper is twofold: Gain a better understanding of the speed changes that did occur during the lockdown, and explore how the data set might be used to model the relationship between speed and traffic volume for larger areas.

While Molloy *et al.* (2021) showed that there was an increase in speeds during the lockdown, it is not clear if this happened for all road types in Switzerland in a similar manner. Regarding the relationship between traffic volumes and speed, the data set might be useful since it includes a larger variance in traffic volumes and possibly speeds than would be seen in a setting without a lockdown. As the shape traffic demand might have also shifted drastically during the lockdown, accounting for different road types is interesting, as it makes sure the association between traffic volume and speed is not an artifact of people using higher-speed roads (e.g. motorways) during the low-traffic lockdown. Nonetheless, it is not clear that the demand during the two phases was comparable, hence it is interesting to investigate whether any association between speeds and traffic volume is different for the baseline and lockdown. Lastly, it is worth wile to see how this modelling works for larger areas, as this might indicate in which cases the data could be used for estimating MFDs in future research.

Based on these considerations, the following three research hypotheses were formulated:

- **Hypothesis 1:** During the lockdown, speeds increased on all road types in Switzerland.
- **Hypothesis 2:** When combining the data for the baseline and lockdown periods, the association between traffic volume and spatial average speeds is significant, even when adjusting for different road types.
- **Hypothesis 3:** There is no evidence that the association between traffic volume and spatial average speed was different for the baseline and lockdown periods.

A brief overview of the scope of the data set is provided in chapter 2. Issues of data quality are considered, and possible explanations are investigated. In the end of the chapter, the data cleaning methods applied will be given. Chapter 3 describes the methods used for data aggregation and modelling. The results of these models are given in chapter 4. A discussion and conclusion is then provided in chapter 5.

2 Data quality

2.1 Background and scope of the data

The data used in this paper was obtained in the context of the MOBIS mobility study conducted by IVT in fall of 2019. In order to assess the impact of different mobility pricing schemes on transport behavior, the movement data of study participants was recorded over three months using app-based GPS tracking.

At the advent of the COVID-19 lockdown in Switzerland, participants of the study were asked to reactivate the tracking app. Consequently, the data set comprises the movement data for study participants for both a reference period in fall of 2019, as well as their behavior during the lockdown and in many cases even beyond.

In terms of geographic distribution, the data contains observations centering around the largest cities of Switzerland, namely Zürich, Bern, Basel, Lausanne and Geneva. This can be seen in figure 1. A particularly high number of observations were made in the city of Zürich.

The temporal scope of the data is a period ranging from September 2019 until March 2021. The number of participants actively tracking their movements was not constant over this period, as can be seen in figure 2. Users were considered to be active users on any given day if they had recorded observations within the preceding or following seven days. By far the highest number of active users was achieved in fall of 2019, with over 2500 active users. A further peak can be observed at the beginning of the COVID-19 lockdown, when users were asked to reactive the tracking.

Figure 1: Spatial distribution of observations: The number of observations made in each Swiss municipality is displayed using a logarithmic scale.

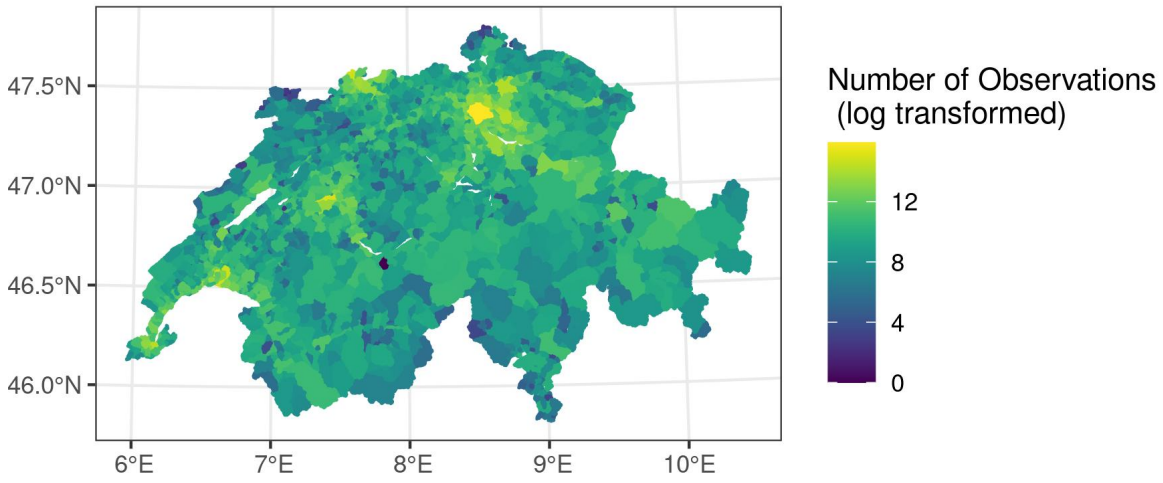

Source: MOBIS-Covid, Swiss municipalities from Federal Statistical Office (BFS) (2020)

2.2 Possible issues with the data

The GPS points obtained in the tracking were then map-matched by IVT to the open street map network of Swiss roads. By considering link length, entry and exit times, it was then possible to calculate for each link crossed by a participant the speed at which they traversed the link. Consequently, the data can be considered floating car data providing information about traffic speeds on large portions of the Swiss road network over long periods of time.

An initial assessment of the data brought to light some issues concerning the distribution of link speeds, link durations and trip speed patterns. Their nature and possible explanations will be discussed in this chapter.

Figure 2: Daily active users and daily legs per active user: For the period of available data, the total number of daily active users and the number of trips per active user is given as a 7 day rolling mean.

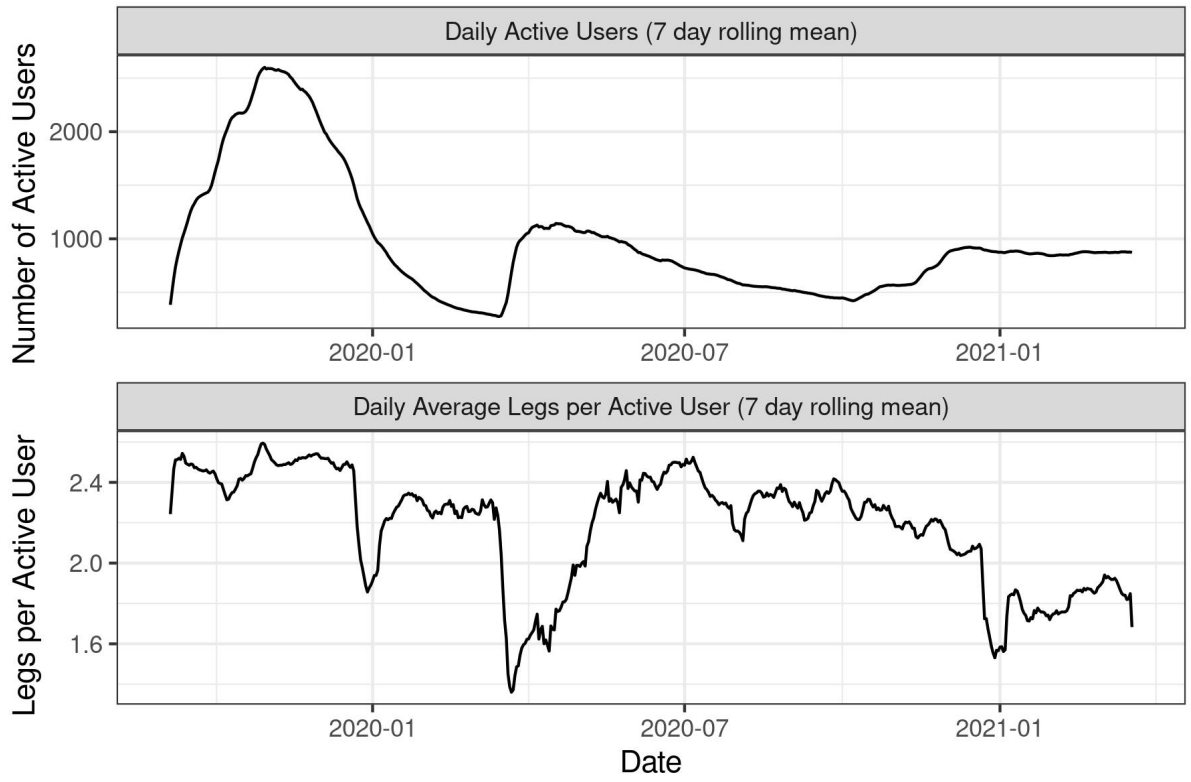

Source: MOBIS-Covid

2.3 Link speed distribution

The most obvious issue with the map matched data was the distribution of link speeds. As can be seen in figure 3, the link speeds have a heavy tail, with 9% percent of them having observed speeds over 180km/h. This is well beyond the maximum legal speed limit on Swiss roads of 120km/h, and therefore indicates issues with the data.

In the following subsections, it is attempted to discover any characteristics shared by these high speed ($>$ 180km/h) observations, which might explain their occurence.

Figure 3: Link speed distribution: The relative frequency of speeds in the data.

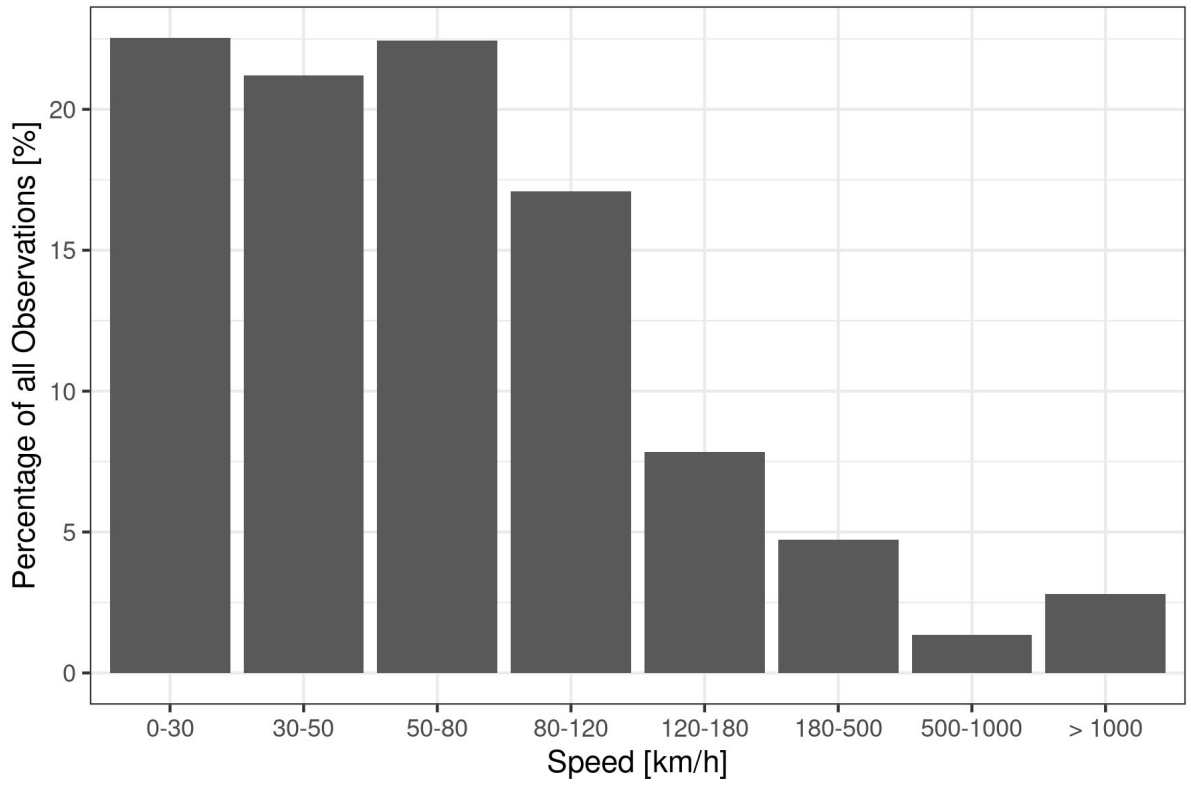

Source: MOBIS-Covid

2.3.1 High speeds by link length or road type

An initial suspicion was that these high speeds occurred predominantly on short links. This was motivated by the fact that the map matching only used GPS points with a certain distance between them, which might lead to issues when mapping to links shorter than the distance between two GPS points.

However, the results in figure 5 suggest that this is not the case. The percentage of observations with speed over 180km/h is smallest for links with distance under 100m, and increases slightly with increasing link length. This increase is most likely due to the lower number of long links. Overall, no group shows large deviations from the global average of 9% of links over 180km/h.

A subsequent hypothesis that specific road types were more prone to issues with speed measurement also was rejected. The results in figure 5 show that while motorway links

Figure 4: Frequency of high speeds by link length: The percentage of observations over 180km/h out of all observations is given for different link lengths.

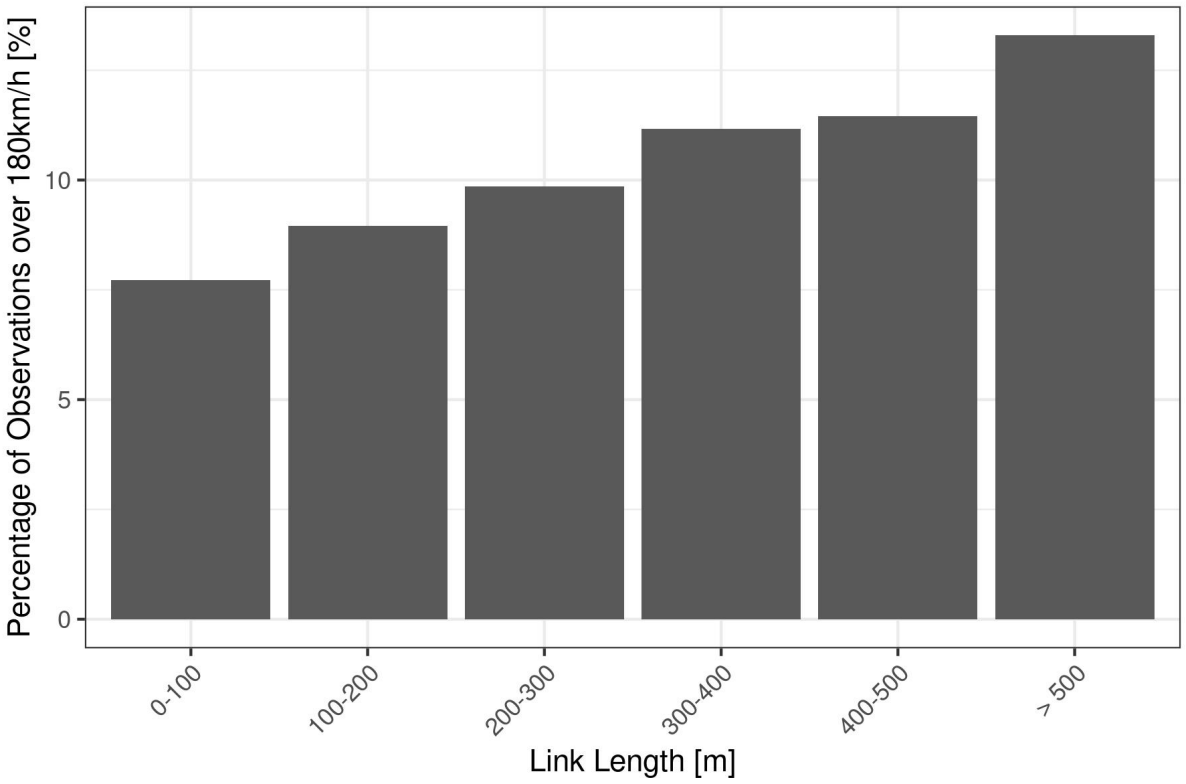

Source: MOBIS-Covid

seem to be the most susceptible, all other road types also had values close to the global mean. Consequently, the phenomenon of high speeds did not occur solely on a specific road type.

A possible relation between high speeds and tunnels was also investigated, but did not yield conclusive results. The different types of tunnels and galleries did have a higher share of observations with speeds over 180km/h (up to 25%). But observations on these links accounted for less than 2% of all observations, meaning that a large part of the high speeds happened on other kinds of links.

Figure 5: Frequency of high speeds by link type: The percentage of observations over 180km/h out of all observations is given for different link types.

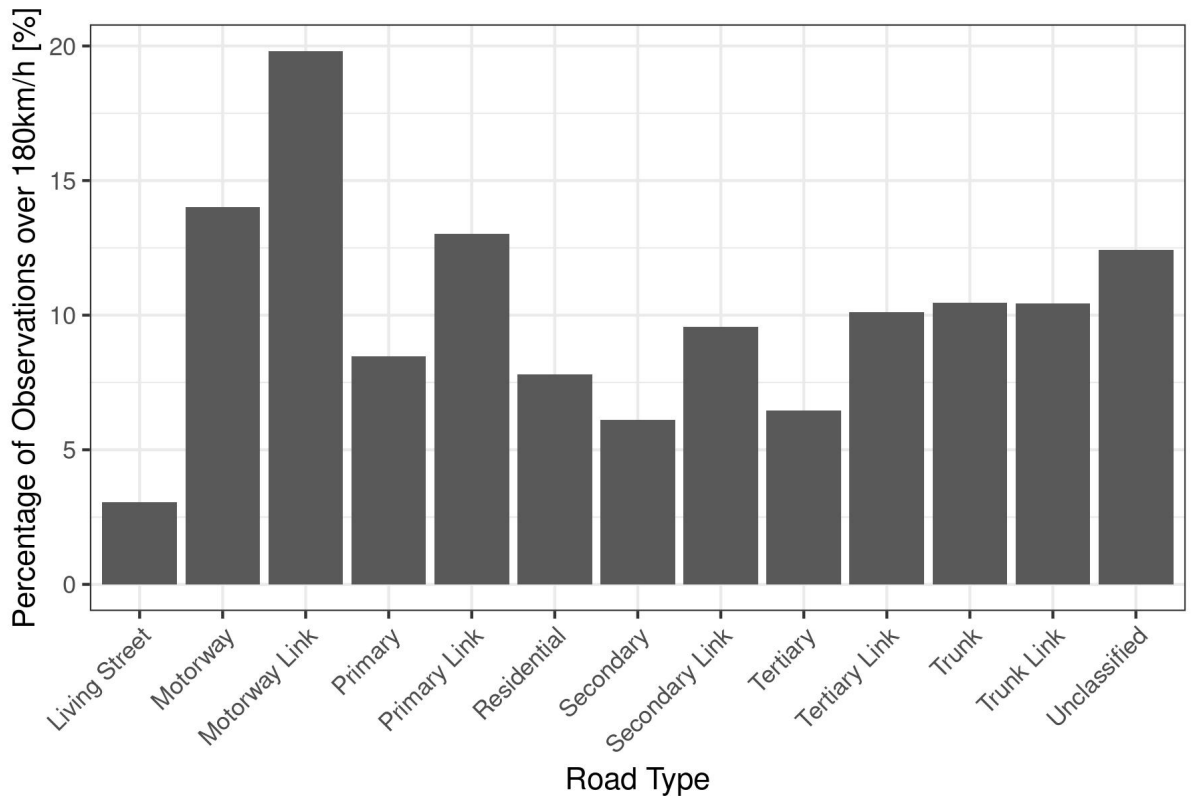

Source: MOBIS-Covid

2.3.2 Geographic distribution of high speed observations

In figure 6, it becomes clear that the high speed obervations are distributed homogeneously across Switzerland. The municipalities with very high percentages are sparsely populated areas with few observations, explaining the high percentages. Considering the main urban centers, the percentage of high speeds appears to be close to the global mean of 9% throughout.

2.3.3 Illustration of possible issues

In order to gain a better understanding of what might be happening with the map matching, random trips involving high speeds were plotted spatially. Two of these were selected to illustrate possible issues with the map matching. They merely serve as indicator

Figure 6: Spatial distribution of high speeds: For each Swiss municipality, the percentage of observations with speed over 180km/h is shown.

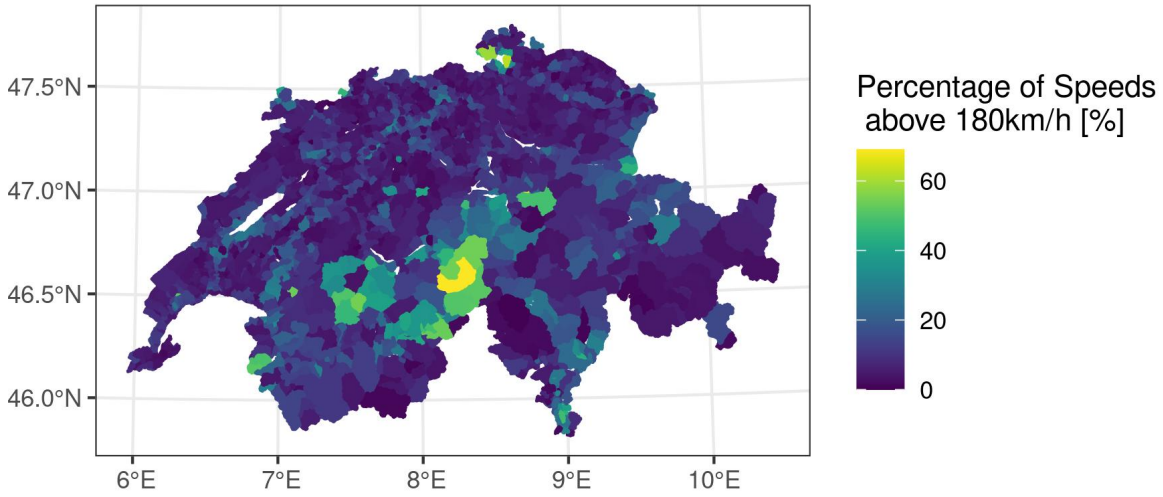

Source: MOBIS-Covid, Swiss municipalities from Federal Statistical Office (BFS) (2020)

of possible issues, and are not representative.

The trip shown in figure 7 shows that the high speeds are potentially connected to errors in the map matching. The majority of the trip has sound speeds, but there is one stretch where speeds are much higher. This stretch coincides with a detour where the map matched path deviates from the highway and goes onto local roads. A possible explanation might be that the participant was travelling along the highway, and the map matching partially assigned the points to the local road. Subsequently, the map matching suggests larger distances covered in the same amount of time, leading to high speeds.

The fact that the high speeds in figure 7 are all within a loop might point to a possible filtering method involving the graph topology of the trip, where trips with loops or repetitive use of links are excluded. However, the overall structure of the shown trip is itself a loop, showing that such filtering might also eliminate correctly matched trips

Figure 7: Spatial representation of a trip: For one trip involving speeds over 180km/h (trip ID 17555313), the link observations and corresponding speeds are plotted spatially. Start and end points of the trip are marked.

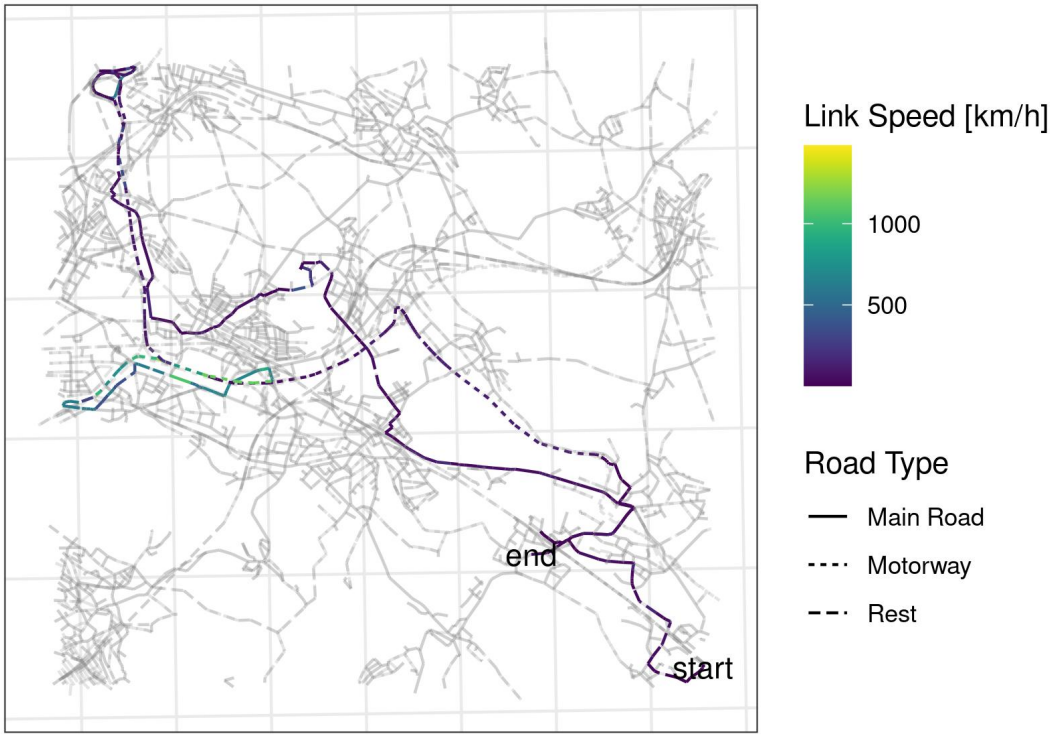

Source: MOBIS-Covid

Finally, the trip shown in figure 8 shows that these probable map matching errors are not the only reason for high speeds. While the maximum speeds in this case are much lower than in figure 7, a speed of over 200km/h on a main road is still implausible.

In this case, there is no obvious explanation for the high speeds. The trip is contains no unnecessary loops or deviations. Furthermore, the trip did not exhibit the freeflow speed imputation pattern discussed in the following subsection, which could explain such speeds.

2.4 Freeflow speed imputation

Another issue uncovered during initial data assessment was the effect of speed imputation. During the map matching, a low number of GPS points can lead to the trip speeds being

Figure 8: Spatial representation of a trip: For one trip involving speeds over 180km/h (trip ID 22336285), the link observations and corresponding speeds are plotted spatially. Start and end points of the trip are marked.

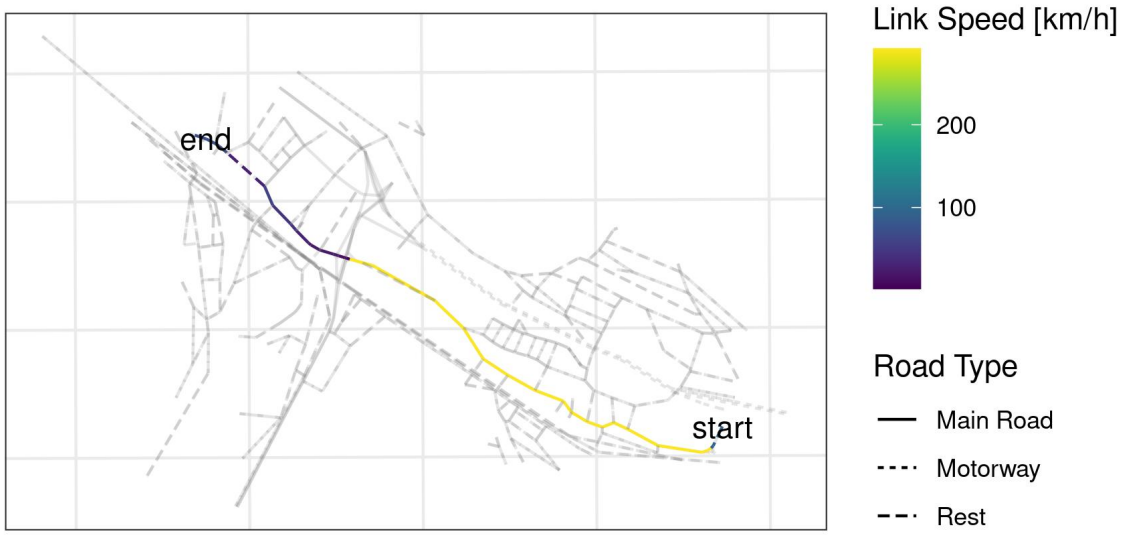

Source: MOBIS-Covid

imputed using the freeflow speeds of the links and scaling accordingly. An example of this is given in figure 9, where the observed speeds are clearly the freeflow speeds scaled by a constant factor. The resulting speeds are implausible.

2.5 Link duration distribution

For a small number of observations, the link durations observed were also deemed implausible. Looking at table 1, some of the trips had durations of up to 22 hours.

Figure 9: Speed of a trip with imputation: For a trip (trip ID 11386989), the link speeds and freeflow speeds as given by open street map are plotted against time.

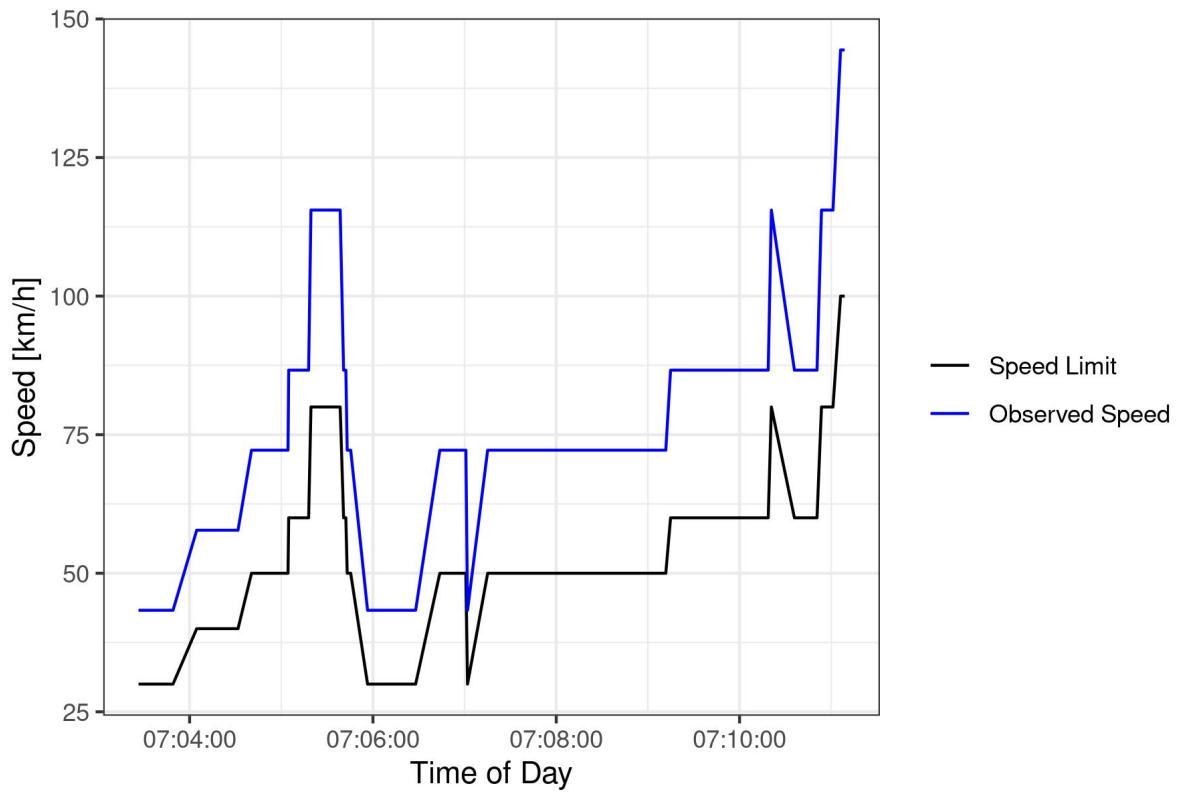

Source: MOBIS-Covid

Table 1: Table showing the summary statistics of the link duration (i.e. the number of minutes each observation took to cross the link).

Min.	1st Qu.	Median	Mean	3rd Qu.	Max.
0.00	0.03	0.10	0.30	0.23	1335.03

Source: MOBIS-Covid

2.6 Data cleaning applied

In light of the low plausibility of some observations, the data was filtered according to the following criteria:

- Any observations with link speeds over 180km/h were filtered (9% of observations)
- Any trips for which the variance of the ratio between observed link speed and freeflow link speeds was smaller than $2.2 \cdot 10^{-4}$ were filtered (less than 1% of observations)

- Any observations for which the link duration was over 3h was eliminated (less than 1% of observations)

3 Methods

3.1 Approaches considered

The modelling involved aggregation of the data for different spatial scales. At first, models aggregating the data by road type for the entire observed area (i.e. large parts of Switzerland) were considered. In a next step, similar methods were applied to smaller scale areas, notable large cities and cantons. The methods used for these models are described here. Lastly, an attempt was made to aggregate the data separately for smaller cities too. This gave rise to issues with the data, and the approach was not developped further. Nevertheless, a brief overview is given in appendix A.

3.2 Countrywide model

3.2.1 Temporal constraints

The analysis was limited to the periods between September 16 and December 1 2019 for the baseline, and between March 26 and April 26 2020 for the lockdown. The periods were selected such that each day had at least 1200 active users, and the large drop in traffic demand during the lockdown would be covered (compare figure 2). The data was limited to working days during the timeframe considered, and public holidays were omitted.

Since the difference in speeds during the lockdown compared to the baseline was most pronounced during the rush hour periods in Molloy *et al.* (2021), only observations during the rush hours (6:30-8:30 AM, 4:30-6:30 PM) were considered. The two rush hour periods (morning and evening) were considered separately.

Table 2: Description of the road type classification used.

Given name	**Relevant categories in OSM**	**Description**
motorway	motorway, motorway_link	includes the Swiss motorways (Autobahnen)
main_overland	primary, primary_link, trunk, trunk_link, secondary, secondary_link	includes main roads (Hauptstrassen) and trunk roads (Autostrassen) with speed limits above 50km/h
main_urban	primary, primary_link, secondary, secondary_link	includes main roads (Hauptstrassen) with speed limits smaller than or equal to 50km/h
side_overland	tertiary, tertiary_link, unclassified	includes any other roads with speed limits above 50km/h
side_urban	tertiary, tertiary_link, unclassified, residential, living_street	includes any other roads, residential streets and living streets (Begegnungszonen) with speed limits smaller than or equal to 50km/h

3.2.2 Spatial constraints

The data considered was limited to observations conducted within Switzerland. As can be seen in figure 1, the majority of these observations occurred in the major urban areas. Hence, the models are not necessarily representative for more rural our mountainous regions.

3.2.3 Road type classification

The road type classification used in this model was based on the data provided by the OSM network (OpenStreetMap contributors (2021)). As the road classification provided by OSM focuses solely on road hierarchy and does not provide context on the location of the road, the classification system was modified. For roads other than motorways, a distinction between urban and overland roads was introduced based on the speed limit. The trunk roads were grouped with the primary roads and not with the motorways as their average speed limit was closer to the main roads than to the highways.

3.2.4 Data aggregation

The raw data was present in a form where each row corresponded to an observation of one user traversing one link. It was aggregated in the following way:

- For each road type, day and rush hour period, calculate the spatial average speed

$$\bar{v} = \frac{\sum_i d_i}{\sum_i t_i}$$

  where for a given observation i, d_i is the length of the link in question and t_i is how long it took the participant to traverse the link
- For each road type, day and rush hour period, calculate the total number of link-level observations NO (i.e. the number of terms in the sums above)
- For each road type, day and rush hour period, calculate the number of distinct users NU (i.e. how many different users were observed in a given period on a given road type)
- Scale both NO and NU by the number of active users on a given day to obtain the scaled number of observations SNO and the scaled number of distinct users SNU

Since the data set did not include absolute traffic levels, the values of SNO and SNU were defined to serve as proxy variables for traffic volume. The scaling was done in order to account for the fact that there were far more active users during the baseline period. During initial modelling, SNU was found to perform better in the models considered. Since SNO and SNU were highly correlated, they could not enter the models at the same time. Hence, the analysis focused on SNU solely.

3.2.5 Data overview

The number of observations NO that go into the calculation of the spatial average speed $\bar{v}$ for a given day and rush hour period can be seen in figure 10. All road type except for the overland side roads have a very high number of observations going into each average.

In figure 11, we can see possible links between the scaled number of distinct users and the spatial average speeds. The baseline period consistently has larger number of scaled distinct users, and also on average lower spatial average speed. Hence for all road types

Figure 10: Distribution of observations by road type: For each road type, the distribution of the number of observations in a rush hour period is given.

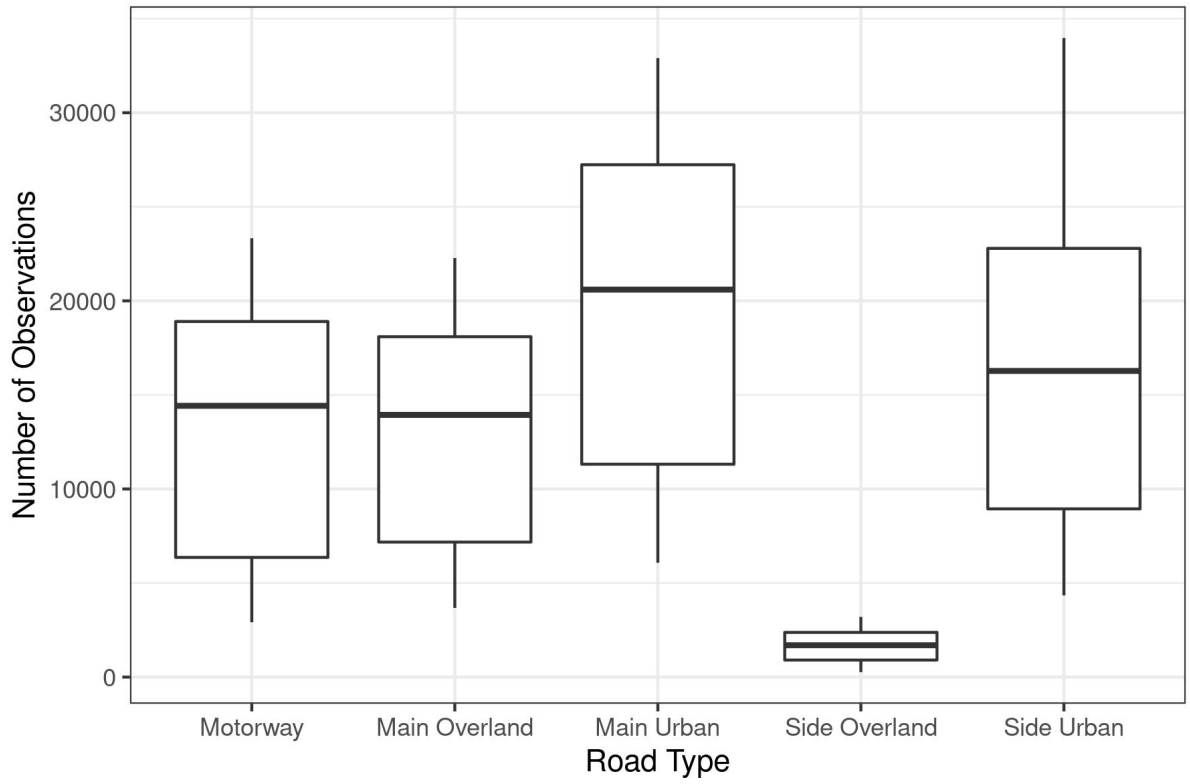

Source: MOBIS-Covid

and rush hour periods, there seems to be a negative correlation when looking at the two pandemic phases combined. When looking at each of the pandemic phases separately, the main roads still seem to exhibit such a pattern. In the case of the motorways and side roads, this is no longer the case.

Another fact that is perhaps interesting to note is how when looking at the number of distinct users, the highways and overland side roads seem to have similar traffic levels. This initially seems contradictory to figure 10, where the overland side roads had far fewer observations. An explanation might be road hierarchy, since a trip can usually involve side roads without involving motorways, but not vice versa. So even if a user conducts most of their trip on a motorway, they will also count as a distinct users for one or more lower road types. Such behavior just goes to show that the scaled number of distinct users is not a perfect proxy for traffic volume or density.

With regards to modelling, figure 11 points to two possible issues: There seems to be

more scatter for higher speeds, and the overland side roads seem to have larger variance than the other road types. Larger absolute deviations for higher speeds is not surprising, and the high variance for overland side roads might be attributed to the low number of observations on these. After initial modelling and consideration of the residual plots, it was found that overland side roads did have larger residual variance. Consequently, this category was excluded from the models. To address the heteroscedasticity observed with the speeds, all models were fit with a log-transform of both the speed and *SNU* variables. This improved the residual plots, and was therefore the approach used in all models.

3.2.6 Models fitted

For each of the rush hour periods separately, three distinct models were fitted. The first model only includes the road type and the lockdown phase indicator in order to investigate the first hypothesis. The regression equation corresponding to this RT (road type) model can be seen in equation 1.

$$\begin{aligned}\log(\bar{v}) =& \beta_0 + \beta_{MO}\chi_{MO} + \beta_{MU}\chi_{MU} + \beta_{SU}\chi_{SU} + \\ & \chi^{LD}(\beta_0^{LD} + \beta_{MO}^{LD}\chi_{MO} + \beta_{MU}^{LD}\chi_{MU} + \beta_{SU}^{LD}\chi_{SU})\end{aligned} \tag{1}$$

In equation 1, β_0 corresponds to the intercept, the χ are dummy indicator variables for the road type indicated by the subscript or the lockdown in case of χ_{LD}. For the road type, the motorway was chosen as the reference level. The β are the corresponding coefficients to be estimated.

As discussed, the explanatory variable speed was entered with a log-transformation. The model therefore does not model the absolute change in speed during the lockdown, but the relative change in speed compared to the previous levels.

The second model fit, named RTT (road type traffic), includes the road types and the traffic proxy *SNU*. Its equation is given in equatin 2. The road types once again enter as dummy indicator variables, with the motorway being the reference level. An interaction between road type and *SNU* was added, such that there could be different strengths of association between traffic and speed for the different road types. The lockdown did not

Figure 11: Scaled number of distinct users and spatial average speeds by road type: For each road type and rush hour period, the number of scaled distinct users and spatial average speeds are shown, with pandemic phases indicated by color.

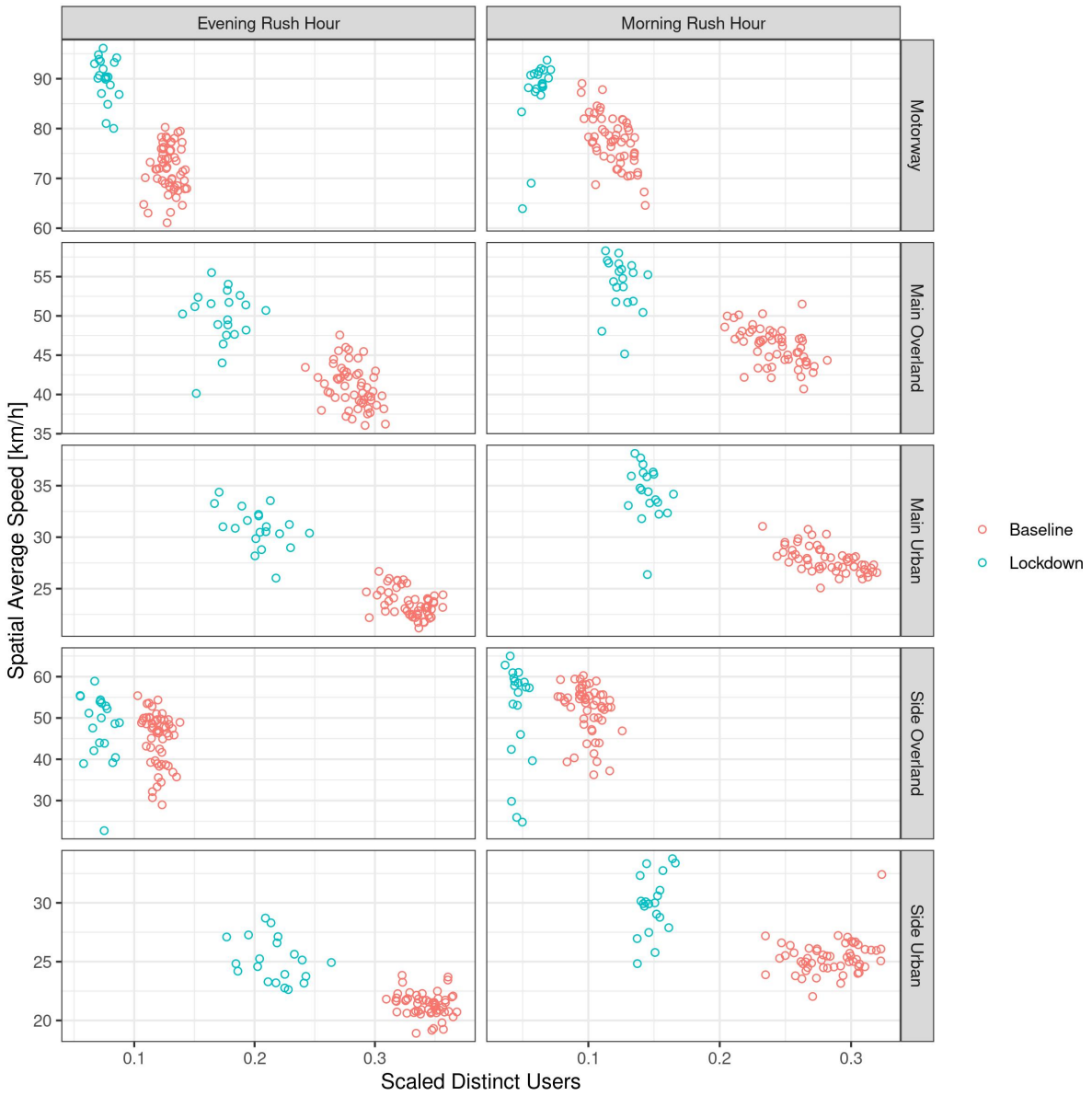

Source: MOBIS-Covid

enter the model, hence the data was essentially pooled and could provide an answer on the second hypothesis.

$$\begin{aligned}\log(\bar{v}) =& \beta_0 + \beta_{SNU}\log(SNU) + \\ & \beta_{MO}\chi_{MO} + \beta_{MU}\chi_{MU} + \beta_{SU}\chi_{SU} + \\ & \log(SNU)(\beta_{MO}^{SNU}\chi_{MO} + \beta_{MU}^{SNU}\chi_{MU} + \beta_{SU}^{SNU}\chi_{SU})\end{aligned} \tag{2}$$

Finally, the third model fit, named RTLDT, extends the RTT model by allowing for different SNU coefficients for the baseline and lockdown periods (see equation 3). This is done by including the β_{LD}^{SNU} coefficient. Thus, there will be the possibility for different associations of $\bar{v}$ and SNU for the different pandemic phases, and the model can give an insight on the third hypothesis.

$$\begin{aligned}\log(\bar{v}) =& \beta_0 + \beta_{SNU}\log(SNU) + \beta_{LD}\chi_{LD} + \\ & \beta_{MO}\chi_{MO} + \beta_{MU}\chi_{MU} + \beta_{SU}\chi_{SU} + \\ & \log(SNU)(\beta_{MO}^{SNU}\chi_{MO} + \beta_{MU}^{SNU}\chi_{MU} + \beta_{SU}^{SNU}\chi_{SU} + \beta_{LD}^{SNU}\chi_{LD})\end{aligned} \tag{3}$$

3.3 Regional models

In addition to the countrywide models, models were fitted for smaller spatial areas. The motivation for this was that in MFD models, homogeneity of the traffic in the region considered is an important requirement. Albeit them not being MFDs, it is still possible that the models fitted here would improve too with spatial homogeneity of traffic. Nonetheless, less aggregation of the data might also increase the variance of the averages, and hence lead to poorer model performance.

3.3.1 Temporal constraints

The temporal constraints for the regional models were the same as the ones used for the countrywide models.

3.3.2 Spatial constraints

So as to avoid issues caused by having too little data, the modelling was limited to the two cities with the highest number of observations: Zürich and Bern. Additionally to both of these cities, their corresponding cantons were chosen as a further region (where the cities did not form subsets of the cantons). In other words, an observation either counted in the city of Zürich, or in the canton of Zürich without the city, but not in both. Further cities were considered, but even for the city with the next-highest total number of observations, Lausanne, some road types had less than ten observations for a rush hour period stemming from two or less distinct users. Such low number of observations were deemed unfit for modelling.

3.3.3 Road type classification

Due to the smaller regions, the road type classification was modified so as to avoid rush hour periods with very few observations for a given road type. The overland and urban categories for main and side road were combined, since the cities contained very few observations for overland roads. As before, the overland side roads were fully omitted from modelling. The motorways remained unchanged.

3.3.4 Data aggregation

The data aggregation conducted was largely identical to how it was done for the country-wide models. The only difference was that additionally to grouping the observations by day, road type and rush hour period, they were also grouped by the region within which they occurred. For this, each link was assigned to the Swiss municipality in which its starting node lies, and the links were hence grouped into the regions.

Figure 12: Distribution of observations by road type and region: For each road type and region, the distribution of the number of observations in a rush hour period is given.

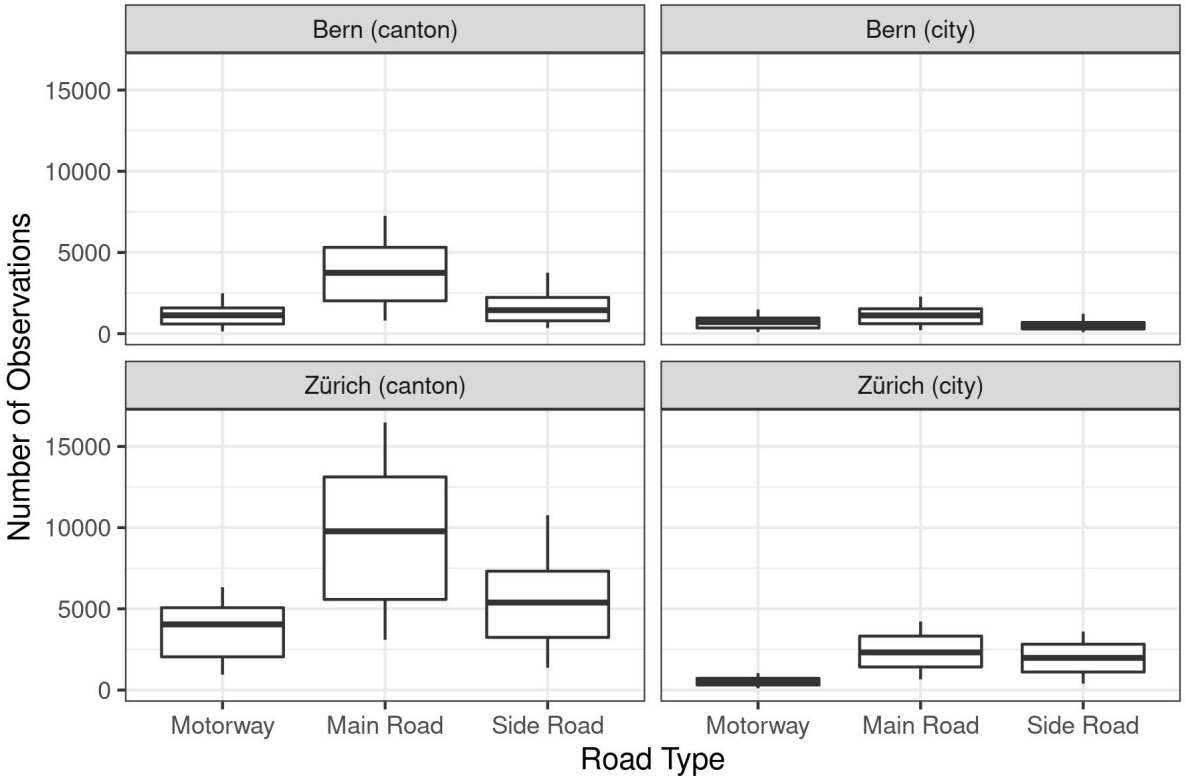

Source: MOBIS-Covid

3.3.5 Data overview

The total number of observations in each region, day and rush hour period and road type is given in figure 13. In all cases, the canton of Zürich had the most observations, followed by the canton of Bern. For the cities, Zürich had more observations than Bern on the main and side roads. For the motorways, Bern seems to have slightly more observations on most days. This might be because Bern has a major motorway fully crossing the city. The rush hour period/road type combinations that had the fewest contributing observation occurred for the city of Bern on motorways and side roads, both having 95 observations.

An overview of the scaled number of distinct users and spatial average speed is offered in figure 13. The perhaps most striking feature is the clear distinction between the motorways and the other road types. As expected, the motorways have consistently higher spatial average speeds. The rush hours during the lockdown phase show lower number of distinct

users for all road types and regions considered. However, the speeds are not always clearly higher during the lockdown. For the city of Zürich for example, the speeds appear higher during the lockdown. This is most prominent for the motorways. In the case of the canton of Bern however, this trend for higher speeds during the lockdown is not as clearly visible.

Considering a possible association between scaled number of distinct users and spatial average speeds, as mentioned in the hypotheses, this appears plausible especially for the city and canton of Zürich, and perhaps the canton of Bern. The city of Bern shows a less pronounced association when looking at both pandemic phases combined. When looking at the data for the baseline and lockdown separately, there is no clear association visible for any of the regions and rush hours considered.

3.3.6 Models fitted

For each of the four regions considered, two models were fitted. The first one only included the road type and scaled number of distinct users. It correpsonds to the RTT model described in section 3.2. The corresponding model equation is given in equation 4. In order to account for differences during the fall vacations during the baseline period, the indicator χ_{VAC} for school vacations in the respective cantons was added. As the road type categories were adjusted, the χ_M and χ_S dummy variables now indicate main and side roads, respectively.

$$\begin{aligned}\log(\bar{v}) =& \beta_0 + \beta_{SNU}\log(SNU) + \beta_{VAC}\chi_{VAC} + \\ & \beta_M\chi_M + \beta_S\chi_S + \\ & \log(SNU)(\beta_M^{SNU}\chi_M + \beta_S^{SNU}\chi_S)\end{aligned} \tag{4}$$

As for the country wide models, a second model was fit for each region that included an interaction effect between the lockdown and the scaled number of distinct users. This model is given in equation 5, and corresponds to the RTLDT model. Due to the coarser road type aggregation, the RT model was not fit for the smaller regions.

Figure 13: Scaled number of distinct users and spatial average speeds by region: For each region and rush hour period, the number of scaled distinct users and spatial average speeds are shown, with pandemic phases indicated by shape and road type indicated by color.

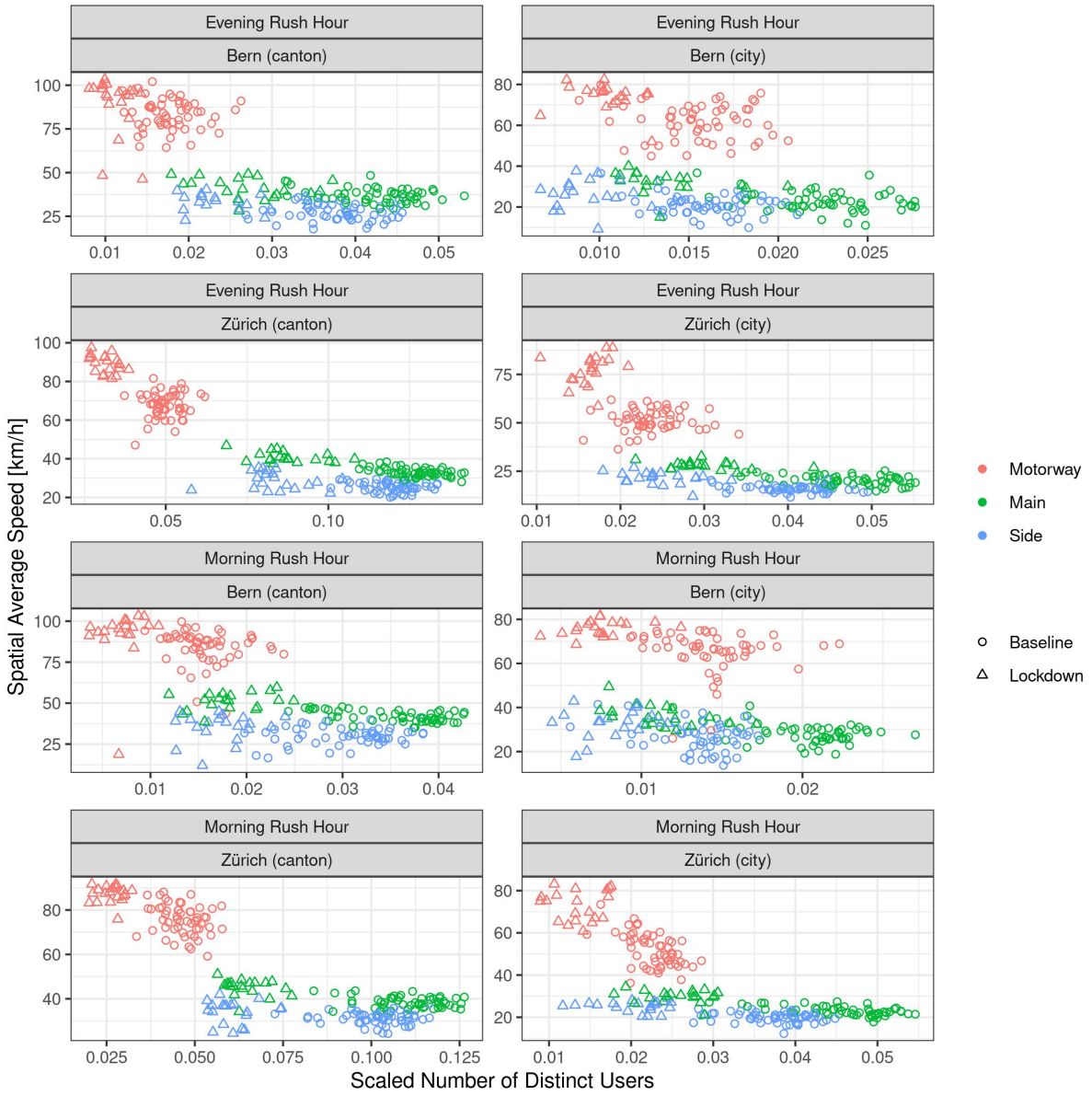

Source: MOBIS-Covid

$$\begin{aligned}\log(\bar{v}) =& \beta_0 + \beta_{SNU}\log(SNU) + \beta_{LD}\chi_{LD} + \beta_{VAC}\chi_{VAC} + \\ & \beta_M\chi_M + \beta_S\chi_S + \\ & \log(SNU)(\beta_M^{SNU}\chi_M + \beta_S^{SNU}\chi_S + \beta_{LD}^{SNU}\chi_{LD})\end{aligned} \tag{5}$$

4 Results

4.1 Countrywide models

An overview of the coefficient estimates for the different countrywide models fitted can be seen in tables 3 and 5 for the morning and evening rush hours respectively. Looking at the RT model in table 3 first, one notes that all road types have lower transformed spatial average speeds for the baseline period than the reference category motorways. This is unsurprising and matches intuition. Furthermore, it can be concluded from the interaction coefficients with the lockdown that the speed increase during the lockdown morning rush hours was significantly more pronounced for the urban main roads than for the motorways, because β_{MU}^{LD} is significant. All other road types did not have significantly different speed increases from the reference category motorway for the lockdown morning rush hours.

In order to compare whether the speeds during the lockdown were significantly higher for all road types, as was conjectured in hypothesis 1, table 4 shows the significance tests for the lockdown effect for all road types. The parameter β_0^{LD} corresponds to the increase in $\log(\bar{v})$ during the lockdown for motorways. Each of the sum of parameters $\beta_0^{LD} + \beta_{\cdot}^{LD}$ then corresponds to the speed increase during the lockdown for the non-reference categories. It is evident that the relative speed increase for morning rush hours was significant on all road types considered. The effect was most pronounced for main urban road, and (relative to previous levels) least pronounced on motorways. Hence, hypothesis 1 holds true for the morning rush hour period.

A look at the RT models for the evening rush hour in table 5 also shows that all road types had significantly lower baseline speeds than the reference category. In this case however, the difference between the speed increase during the lockdown for motorways

and main urban roads was less significant. On the urban side roads, the relative speed increase was significantly less pronounced than for the motorways. Again comparing the difference between the lockdown and baseline periods shown in table 6, all road types had significantly higher speeds during the lockdown period. As in the morning rush hour, the difference was the largest for the main urban roads. Consequently, hypothesis 1 also holds true for the evening rush hour.

The RTT model for the morning rush hour in table 3 reveals that the traffic proxy $\log(SNU)$ has a significant association with the transformed spatial average speed. Since this model pooled the data for the baseline and lockdown periods and accounts for road types, the significant β_{SNU} parameter confirms hypothesis 2 for the morning rush hour. When looking at the different road types, the slopes of the best fit lines on the log-transformed variables differ significantly from the reference category motorway in some cases. Especially the main urban roads have a steeper negative slope in the transformed space, indicating that the main urban roads' speeds react more sensitively to relative changes in traffic volume than the motorways.

To assess hypothesis 3 for the morning rush hour periods, it is necessary to consider the RTLDT model. The significant β_{LD}^{SNU} parameter suggests that the association between the scaled number of distinct users and the spatial average speeds was different for the baseline and lockdown periods, thereby confirming hypothesis 3 for the morning rush hours. When looking at the effect of the scaled number of distinct users for the different road types, it is interesting to note that for the urban and overland main roads, the parameters have different signs when compared to the RTT model. This might be an indication that the different road types acted differently during the lockdown.

Lastly, the RTT and RTLDT models for the evening rush hour in table 5 are in agreement with the ones for the morning rush hour concering the hypotheses. The β_{SNU} parameter is significant for the RTT model, and β_{LD}^{SNU} is not significant for the RTLDT model. However, it should be noted that for the RTLDT model, the β_{SNU} parameter was not significant. That is, the model did not find any significant association between the scaled number of distinct users and the spatial average speeds in the baseline period. In this case, the $\beta_{\cdot}^{SNU}$ coefficients capturing the change in association strength between speed and traffic between the reference category motorway and the other road types are only significant for the main urban roads, and have the same sign in both models.

Table 3: Estimated parameters of the countrywide models for the morning rush hour period.

	RT (morning)	RTT (morning)	RTLDT (morning)
β_0	4.35^{***}	3.98^{***}	3.68^{***}
	(0.01)	(0.05)	(0.15)
β_0^{LD}	0.12^{***}		0.62^{***}
	(0.02)		(0.13)
β_{SNU}		-0.17^{***}	-0.31^{***}
		(0.02)	(0.07)
β_{MO}	-0.52^{***}	-0.49^{***}	-0.03
	(0.01)	(0.07)	(0.14)
β_{MU}	-1.02^{***}	-1.06^{***}	-0.54^{***}
	(0.01)	(0.06)	(0.15)
β_{SU}	-1.12^{***}	-1.02^{***}	-0.49^{**}
	(0.01)	(0.07)	(0.16)
β_{MO}^{LD}	0.04		
	(0.02)		
β_{MU}^{LD}	0.09^{***}		
	(0.02)		
β_{SU}^{LD}	0.05		
	(0.02)		
β_{MO}^{SNU}		-0.07^{*}	0.19^{**}
		(0.03)	(0.07)
β_{MU}^{SNU}		-0.14^{***}	0.17^{*}
		(0.03)	(0.08)
β_{SU}^{SNU}		-0.05	0.28^{***}
		(0.03)	(0.08)
β_{LD}^{SNU}			0.26^{***}
			(0.06)
R^2	0.98	0.98	0.98
Adj. R^2	0.98	0.98	0.98
Num. obs.	300	300	300

$^{***}p < 0.001$; $^{**}p < 0.01$; $^{*}p < 0.05$

Source: MOBIS-Covid

Table 4: Linear hypothesis tests assessing the impact of the lockdown for different road types during the morning rush hour. All hypotheses are tested with respect to the null hypothesis that the sum of parameters is zero.

	Estimate	Std. Error	t-value	p-value
β_0^{LD}	0.117	0.017	7.055	< 0.001
$\beta_0^{LD} + \beta_{MO}^{LD}$	0.159	0.017	9.567	< 0.001
$\beta_0^{LD} + \beta_{MU}^{LD}$	0.21	0.017	12.662	< 0.001
$\beta_0^{LD} + \beta_{SU}^{LD}$	0.162	0.017	9.797	< 0.001

Source: MOBIS-Covid

4.2 Regional models

As before, the results for the regional models are given separately for the morning and evening rush hours in tables 7 and 8. Focussing first on the morning rush hour, it is interesting to note that the parameters β_{SNU} are significant in three of the four models fit without lockdown interaction. Hence, in three out of four cases, hypothesis 2 is supported. As soon as one allows for different association strengths for the two phases (i.e. different slopes for the baseline and lockdown), this relation is much less pronounced. For the models that did include the lockdown interaction, the fact that the β_{LD}^{SNU} parameters are not significant suggests that the association between traffic volume and speed did not change from the baseline to the lockdown. This means hypothesis 3 can be confirmed. However, since the β_{SNU} parameters were mostly insignificant anyways, it is unclear if the models captured any relationship that could have changed in the first place.

The road type intercepts were significantly different to the reference category when the lockdown was not included in all regions but the city of Zürich. This might be explained by the fact that most of the motorways in Zürich have speed limits below 120km/h, hence making the difference between the reference category and the other road types smaller. Upon inclusion of the lockdown variables, these road type specific intercepts became less significant. This might be related to the fact that the β_{SNU} variables were less significant too in that case. When it comes to the question whether the relation between traffic and speed was different for the different road types, the models fail to give a conclusive answer. The β_M^{SNU} and β_S^{SNU} parameters were significantly positive for the city of Zürich in both models fitted. In the other regions, they were either not significant or even significant with negative sign. Overall, this does not allow for hypothesis 3 to be answered conclusively when looking at smaller regions.

Table 5: Estimated parameters of the countrywide models for the evening rush hour period.

	RT (evening)	RTT (evening)	RTLDT (evening)
β_0	4.28***	3.47***	4.08***
	(0.01)	(0.06)	(0.22)
β_0^{LD}	0.22***		0.02
	(0.02)		(0.09)
β_{SNU}		−0.40***	−0.09
		(0.03)	(0.11)
β_{MO}	−0.56***	−0.23**	−0.55**
	(0.01)	(0.08)	(0.18)
β_{MU}	−1.12***	−0.91***	−1.29***
	(0.01)	(0.08)	(0.20)
β_{SU}	−1.22***	−0.77***	−1.15***
	(0.01)	(0.08)	(0.20)
β_{MO}^{LD}	−0.03		
	(0.02)		
β_{MU}^{LD}	0.05*		
	(0.02)		
β_{SU}^{LD}	−0.06**		
	(0.02)		
β_{MO}^{SNU}		0.02	−0.05
		(0.04)	(0.08)
β_{MU}^{SNU}		−0.15***	−0.23*
		(0.04)	(0.10)
β_{SU}^{SNU}		0.06	−0.02
		(0.04)	(0.10)
β_{LD}^{SNU}			−0.06
			(0.05)
R^2	0.99	0.99	0.99
Adj. R^2	0.99	0.99	0.99
Num. obs.	300	300	300

***$p < 0.001$; **$p < 0.01$; *$p < 0.05$

Source: MOBIS-Covid

Table 6: Linear hypothesis tests assessing the impact of the lockdown for different road types during the evening rush hour. All hypotheses are tested with respect to the null hypothesis that the sum of parameters is zero.

	Estimate	Std. Error	t-value	p-value
β_0^{LD}	0.224	0.016	14.094	< 0.001
$\beta_0^{LD} + \beta_{MO}^{LD}$	0.193	0.016	12.179	< 0.001
$\beta_0^{LD} + \beta_{MU}^{LD}$	0.271	0.016	17.078	< 0.001
$\beta_0^{LD} + \beta_{SU}^{LD}$	0.162	0.016	10.175	< 0.001

Source: MOBIS-Covid

Table 7: Estimated parameters of the regional models for the morning rush hour period.

	Zürich (city)	Zürich (canton)	Bern (city)	Bern (canton)	Zürich (city) LD	Zürich (canton) LD	Bern (city) LD	Bern (canton) LD
β_0	1.83***	3.60***	3.43***	4.20***	2.72***	3.96***	3.62***	4.46***
	(0.19)	(0.12)	(0.28)	(0.24)	(0.39)	(0.30)	(0.49)	(0.59)
β_{LD}					0.49	0.12	0.87	0.88*
					(0.30)	(0.21)	(0.57)	(0.44)
β_{SDU}	−0.56***	−0.24***	−0.18**	−0.05	−0.31**	−0.11	−0.13	0.01
	(0.05)	(0.04)	(0.06)	(0.05)	(0.10)	(0.10)	(0.12)	(0.14)
β_M	0.01	−0.58***	−1.62***	−1.29***	0.08	−0.61	−1.33**	−0.63
	(0.24)	(0.16)	(0.39)	(0.34)	(0.36)	(0.31)	(0.45)	(0.52)
β_S	0.07	−0.50**	−1.35**	−1.07**	0.05	−0.51	−1.31**	−0.32
	(0.24)	(0.16)	(0.42)	(0.36)	(0.30)	(0.30)	(0.42)	(0.52)
β_{VAC}	0.05*	0.01	−0.03	−0.00	0.12***	0.03	0.00	0.08
	(0.02)	(0.02)	(0.03)	(0.03)	(0.03)	(0.02)	(0.04)	(0.04)
β_{LD}^{SDU}					0.07	0.01	0.16	0.16
					(0.08)	(0.07)	(0.13)	(0.11)
β_M^{SDU}	0.14*	−0.05	−0.21*	−0.19*	0.22*	−0.02	−0.13	0.02
	(0.07)	(0.06)	(0.09)	(0.09)	(0.10)	(0.11)	(0.10)	(0.13)
β_S^{SDU}	0.23***	0.09	−0.10	−0.03	0.26***	0.13	−0.09	0.20
	(0.06)	(0.06)	(0.09)	(0.09)	(0.08)	(0.11)	(0.09)	(0.13)
R^2	0.94	0.95	0.83	0.83	0.95	0.95	0.83	0.84
Adj. R^2	0.94	0.95	0.82	0.82	0.95	0.95	0.83	0.83
Num. obs.	225	225	225	225	225	225	225	225

***$p < 0.001$; **$p < 0.01$; *$p < 0.05$

For the regional models during the evening rush hour, the relationship between traffic and speed is again significant for most regions when the lockdown is not included. This can be seen in the significant β_{SNU} parameter for all regions but the canton of Bern. Hence, hypothesis 2 can be confirmed in most cases. Upon inclusion of the lockdown, this association fails to be significant for any region considered. In the case of both the city and canton of Zürich, the β_{LD}^{SNU} coefficients are significant, which would contradict hypothesis 3. It is interesting to note that these results happen for the city and canton of Zürich. Due to their geographical proximity, the data for these regions might well show correlation. When it comes to different slopes for the different road types, parametrized by β_{M}^{SNU} and β_{S}^{SNU}, there is no clearly visible trend across the regions. None of the parameters are highly significant.

Table 8: Estimated parameters of the regional models for the evening rush hour period.

	Zürich (city)	Zürich (canton)	Bern (city)	Bern (canton)	Zürich (city) LD	Zürich (canton) LD	Bern (city) LD	Bern (canton) LD
β_0	1.80***	2.78***	2.89***	3.92***	4.49***	4.70***	3.79***	3.97***
	(0.28)	(0.16)	(0.43)	(0.27)	(0.37)	(0.35)	(0.57)	(0.44)
β_{LD}					−0.70*	−0.33*	0.51	0.23
					(0.29)	(0.15)	(0.71)	(0.26)
β_{SDU}	−0.58***	−0.48***	−0.29**	−0.12	0.15	0.17	−0.07	−0.11
	(0.07)	(0.05)	(0.10)	(0.06)	(0.10)	(0.12)	(0.14)	(0.11)
β_M	−0.64	−0.39	−2.12***	−1.08**	−1.79***	−1.56***	−2.05***	−0.91*
	(0.35)	(0.21)	(0.56)	(0.35)	(0.39)	(0.35)	(0.60)	(0.45)
β_S	−0.66	−0.21	−1.41*	−1.70***	−1.56***	−1.31***	−1.51**	−1.53***
	(0.35)	(0.21)	(0.57)	(0.36)	(0.34)	(0.34)	(0.56)	(0.44)
β_{VAC}	−0.02	0.02	0.08*	−0.04	0.10***	0.07***	0.12**	−0.02
	(0.03)	(0.02)	(0.04)	(0.02)	(0.03)	(0.02)	(0.04)	(0.03)
β_{LD}^{SDU}					−0.28***	−0.20***	0.07	0.05
					(0.08)	(0.06)	(0.16)	(0.07)
β_M^{SDU}	−0.02	−0.05	−0.32*	−0.12	−0.25*	−0.33*	−0.28	−0.06
	(0.10)	(0.08)	(0.14)	(0.09)	(0.11)	(0.13)	(0.15)	(0.12)
β_S^{SDU}	0.07	0.17*	−0.07	−0.21*	−0.09	−0.08	−0.10	−0.15
	(0.10)	(0.08)	(0.13)	(0.10)	(0.09)	(0.12)	(0.13)	(0.12)
R^2	0.94	0.95	0.85	0.91	0.96	0.96	0.86	0.91
Adj. R^2	0.94	0.95	0.85	0.91	0.96	0.96	0.86	0.91
Num. obs.	225	225	225	225	225	225	225	225

***$p < 0.001$; **$p < 0.01$; *$p < 0.05$

All of the models fit show R^2 values above 0.8, many even above 0.9. This largely due to the fact that the different road types introduce a large amount of variation in the speeds, which can be easily captured by the road type specific intercepts. Keeping in mind figure 13, it is clear that upon accounting for the different road type, there are still substantial residuals remaining. The diagnostic plots for the models fitted are provided in the appendix. There is some indication that the residuals are not always normally distributed when looking at the Q-Q plots. Otherwise, the diagnostic plots appeared fine. In particular, there is no indication that heteroscedasticity is a serious concern in the models fitted.

5 Discussion and conclusion

The graphs and models presented in this paper allowed for clear conclusions on some of the hypotheses formulated. The countrywide RT models confirm hypothesis 1 and show that spatial average speeds increased on all road types considered. That increase was the most pronounced for main urban roads, both in the morning and evening rush hour periods.

Hypothesis 2 postulated that upon combining the data from the baseline and lockdown periods, the association between the traffic volume and the spatial average speeds is significant. In the case of the countrywide models, this hypothesis can be confirmed. For the smaller spatial regions considered, the effect was only significant for the city and canton of Zürich and the city of Bern. The canton of Bern did not show a significant effect. Overall, there is some evidence in favor of hypothesis 2.

It would be an interesting opportunity for future research to investigate why the effect was present on a countrywide level, but not in the case of the canton of Bern. One possible explanation might be the different road aggregation used for the countrywide and regional models. By grouping both fast overland roads and slow urban roads together, variation in the speeds might become less visible. Furthermore, the coarser aggregation into road types also led to fewer total observations, which would of course lower the power of the hypothesis tests. However, it does not explain why the effect would still be present in the canton of Zurich but not in the canton of Bern.

For hypothesis 3, the models do not allow for a conclusive answer. In both the morning rush hour period for the countrywide model, and the evening rush hour period for the city

and canton of Zurich, there is evidence for different associations between traffic volume and spatial average speed during the baseline and lockdown periods. It must be noted that for the countrywide model, the slope in the transformed space was less negative compared to the baseline, whereas in the two regional models it was more negative. Hence, there is no consistent effect emerging.

The fact that the association of traffic and spatial average speed upon allowing for different slopes in the transformed space was only significant in two models suggests that these models were not adequate to assess the association between traffic and spatial speed in the first place. Hence, it makes sense that they would not provide any strong evidence of different associations. To investigate if and how the change in traffic levels during the lockdown was associated with a shift in the shape of demand, it would be interesting to directly compare trip purposes during the rush hours for the baseline and lockdown periods. If it could be argued that the data for the two pandemic phases indeed is comparable, hypothesis 2 showed that combining the data would then be a viable way to model associations between traffic volume and speeds on larger spatial areas.

While the models did show high goodness-of-fit indicators, this is mostly due to the large variance introduced by the different road types. As can be seen in the plots, there is still substantial variance present in the data. This issue might be mended in future research by finding better ways to filter out implausible observations in the data. While a focus was given to the high speeds in the data quality considerations, another focus might be on the link durations. The cut-off value of two hours chosen might be too high, as most links are under 500m in lengths, and two hours for 500m would correspond to very severe gridlock. Since the spatial average speed was used, there was little robustness against high link duration values, especially for days with few observations.

Another way to improve the modelling would be the inclusion of absolute traffic volume measurements, e.g. by loop detector data. On one hand, it would allow for a more accurate assessment of the traffic situation. On the other hand, it might also allow for the estimation of the probe penetration rate (i.e. what percentage of the cars driving are being measured). This probe penetration rate might help explain differing observations for different regions. It is interesting to note that in the modelling, the countrywide model led to more significant results in most cases (especially with hypothesis 2). This is somewhat surprising, as especially research on the MFD emphasizes the necessity that the traffic in the region considered be homogeneous (compare Ambühl *et al.* (2017)). It would be an interesting research opportunity to investigate why in this case the countrywide models performed better.

6 Acknowledgements

I would like to thank Prof. Dr. Kay W. Axhausen, Thomas Schatzmann and Dr. Georgios Sarlas for both the possibility of writing this thesis at IVT, as well as their many inputs. Furthermore, I extend my thanks to Prof. Dr. Fadoua Balabdaoui for enabling me to pursue this thesis in my application area.

7 References

Aletta, F., S. Brinchi, S. Carrese, A. Gemma, C. Guattari, L. Mannini and S. M. Patella (2020) Analysing urban traffic volumes and mapping noise emissions in rome (italy) in the context of containment measures for the covid-19 disease, *Noise Mapping*, **7** (1) 114–122.

Ambühl, L., A. Loder, M. Menendez and K. W. Axhausen (2017) Empirical macroscopic fundamental diagrams, paper presented at the *TRB 96th Annual Meeting Compendium of Papers*, 17–03331, Washington DC.

de Dios Ortúzar, J. and L. Willumsen (2011) *Modelling Transport*, Wiley, ISBN 9781119993520.

Federal Council (2020) Coronavirus: Federal council declares 'extraordinary situation' and introduces more stringent measures, `https://www.admin.ch/gov/en/start/documentation/media-releases.msg-id-78454.html`.

Federal Office of Public Health FOPH (2020) Table to easing and tightening of nationwide measures, `https://www.bag.admin.ch/bag/en/home/krankheiten/ausbrueche-epidemien-pandemien/aktuelle-ausbrueche-epidemien/novel-cov/massnahmen-des-bundes.html#757183649`.

Federal Statistical Office (BFS) (2020) *Generalised administrative boundaries: geodata*, no. 16804410, Apr 2020.

Harantová, V., A. Hájnik and A. Kalašová (2020) Comparison of the flow rate and speed of vehicles on a representative road section before and after the implementation of measures in connection with covid-19, *Sustainability*, **12** (17), ISSN 2071-1050.

Molloy, J., T. Schatzmann, B. Schoeman, C. Tchervenkov, B. Hintermann and K. W.

Axhausen (2021) Observed impacts of the covid-19 first wave on travel behaviour in switzerland based on a large gps panel, *Transport Policy*, **104**, 43–51, ISSN 0967-070X.

OpenStreetMap contributors (2021) Planet dump retrieved from https://planet.osm.org , `https://www.openstreetmap.org` .

A Panel data methods

As an extension of the regional models, a panel data approach was considered. For this, the data was aggregated in a way similar to how it was done for the regional models. Instead of the four regions described, all Swiss municipalities with more than 200'000 distinct observations within the considered time frame were considered (45 in total). Also, in an effort to avoid issues with too little data especially for small municipalities during the lockdown, the road type distinction was not applied. The approach was then to fit a panel data model where the municipalities corresponded to individuals, and the different dates to the time scale. Morning and evening rush hour periods were considered in separate models. The model considered used a within-transformation that included municpality-specific intercepts and a global slope for the effect of the scaled number of distinct users. (i.e. the traffic proxy).

While the model did show a significant relation between the speed and scaled number of distinct user, an inspection of plots similar to the ones given in 13 gave rise to concerns. Some cities showed a clearly visible link between scaled number of distinct users and the speeds, such as Zürich in figure 13. Other, like Winterthur shown in figre 14 seemed to show a more or less random distribution. This was especially surprising to see for a city like Winterthur, which still had the 8th highest number of observations of any municipality in the sample. Hence, the noise cannot simply be attributed to it being a small town with few observations.

The panel data approach had many advantages. Since the data was less coarsly aggregated, the models had more data and consequently higher power. Furthermore, the different municipalities allowed for a spatial panel data model that accounts for possible spatial correlation between neighboring municipalities to be fit. However, both spatial lag and error autocorrelation were not significant for three different neighborhood matrices considered (distance-based neighbors, k-nearest neighbors and squared inverse free-flow travel time).

These panel data models were ultimately not pursued further due to the issues in the data described above. It would be an interesting opportunity for future research to see whether these issues could be assuaged by using more refined data cleaning techniques. Such a model would offer many benefits like higher power and better justification for the i.i.d assumption.

Figure 14: Scaled number of distinct users and spatial average speeds for Winterthur: For each rush hour period, the scaled number of distinct users and spatial average speeds are shown, with pandemic phases indicated by color.

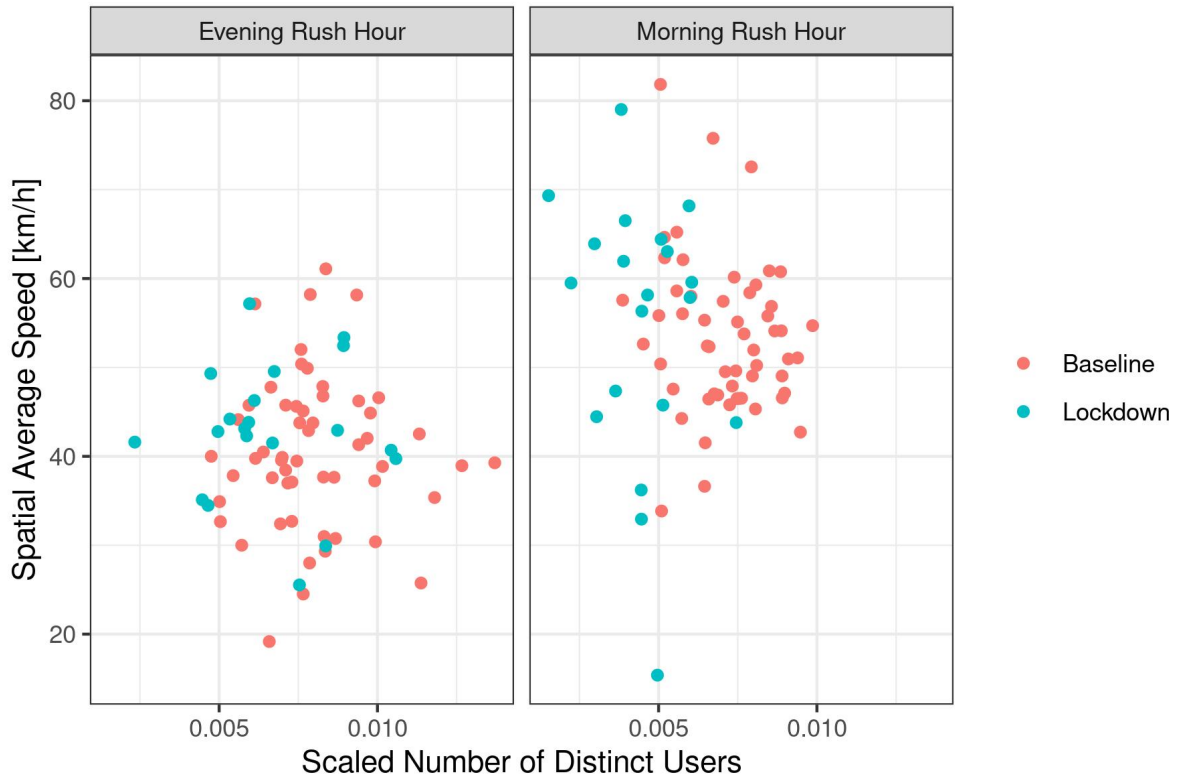

Source: MOBIS-Covid

B Diagnostic plots

Figure 15: Residual, Q-Q and scale-location plot for the RT morning rush hour model.

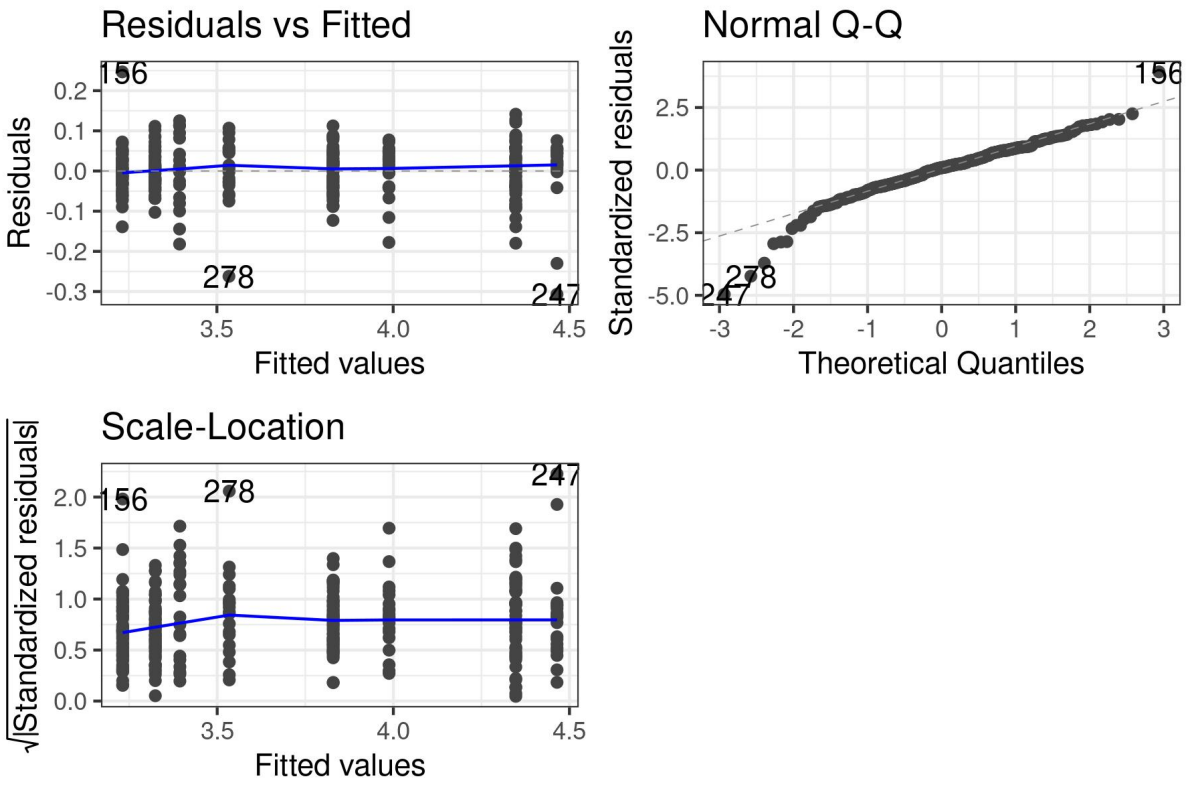

Source: MOBIS-Covid

Figure 16: Residual, Q-Q and scale-location plot for the RT evening rush hour model.

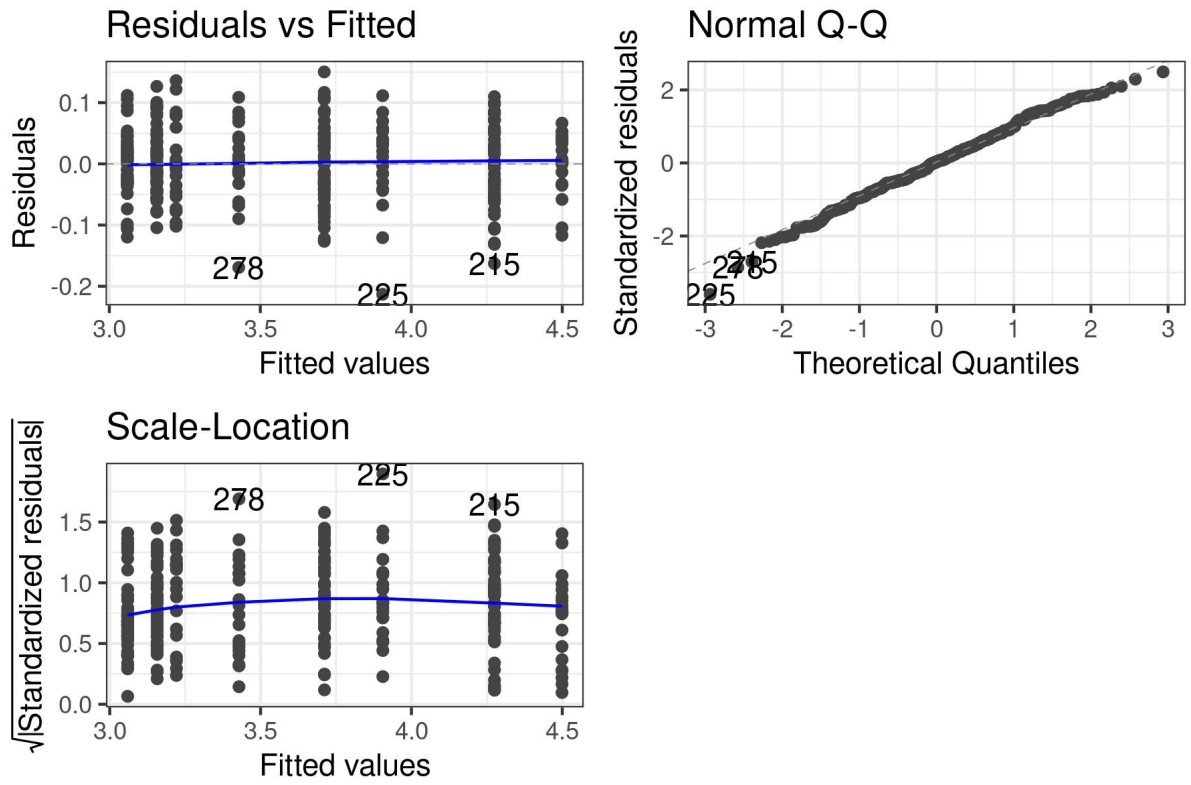

Source: MOBIS-Covid

Figure 17: Residual, Q-Q and scale-location plot for the RTT morning rush hour model.

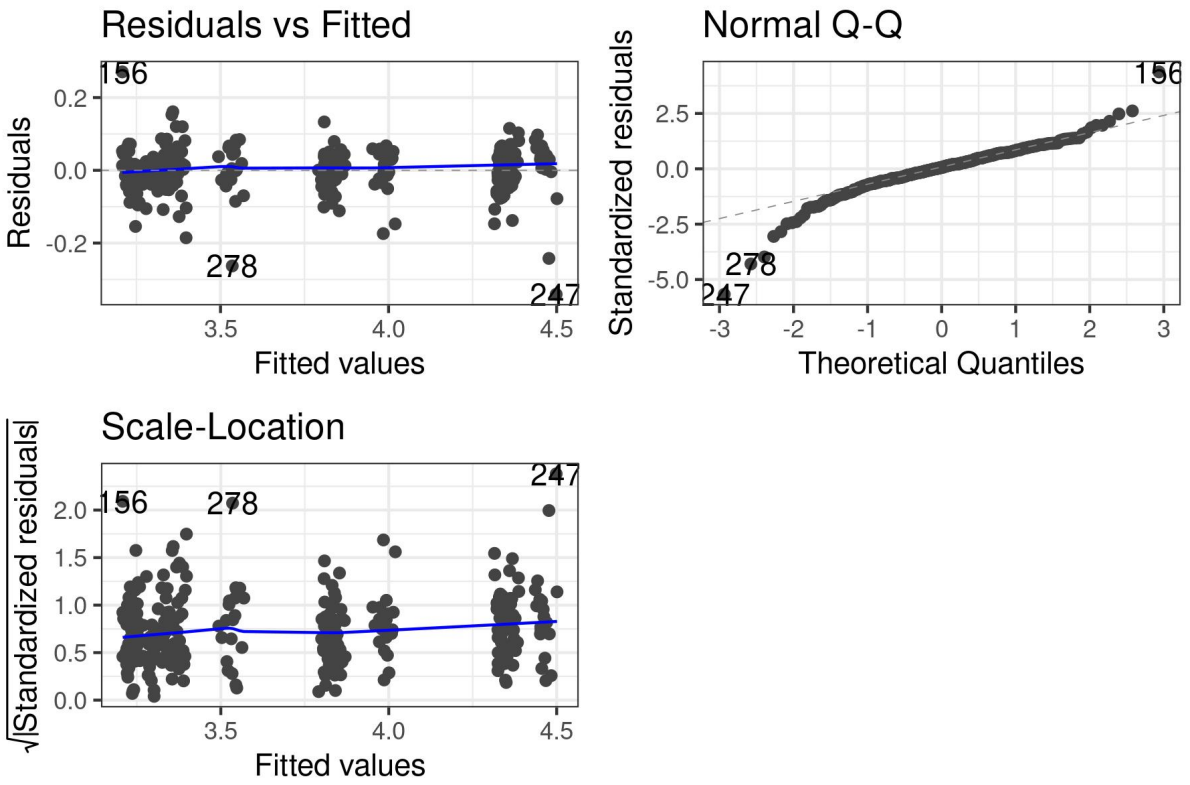

Source: MOBIS-Covid

Figure 18: Residual, Q-Q and scale-location plot for the RTT evening rush hour model.

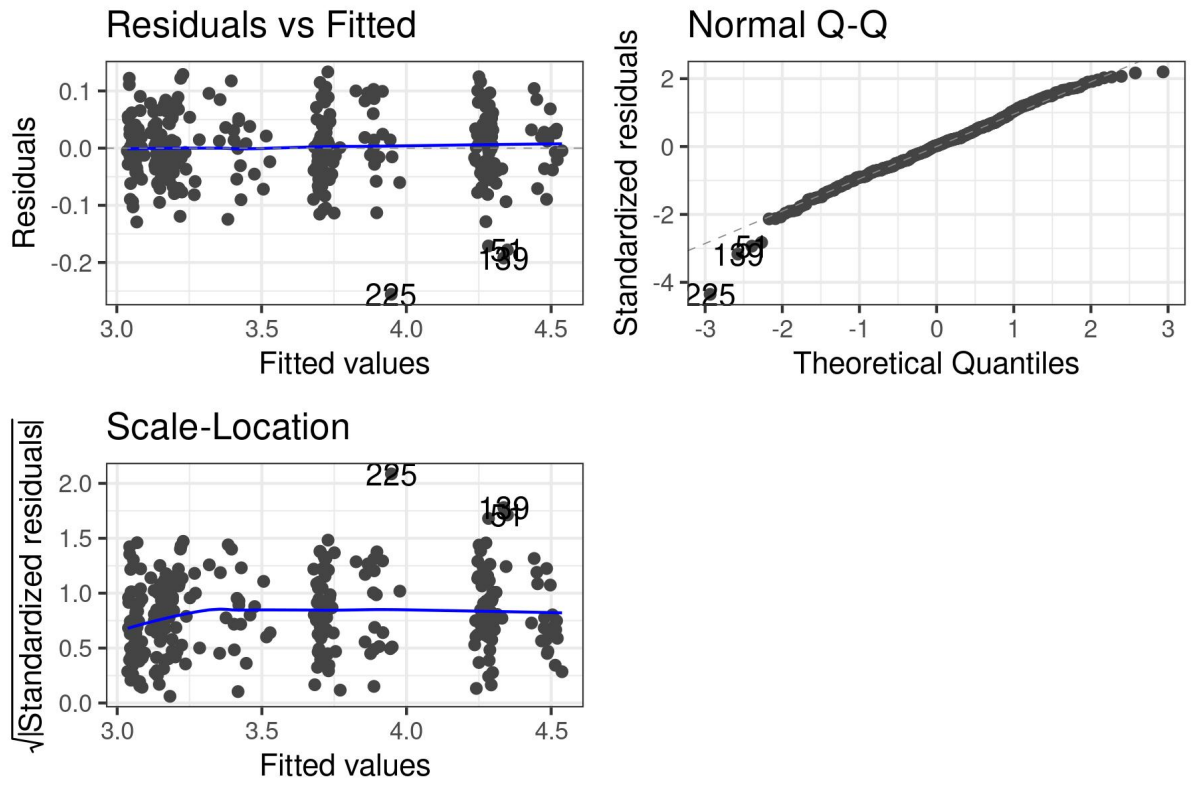

Source: MOBIS-Covid

Figure 19: Residual, Q-Q and scale-location plot for the RTLDT morning rush hour model.

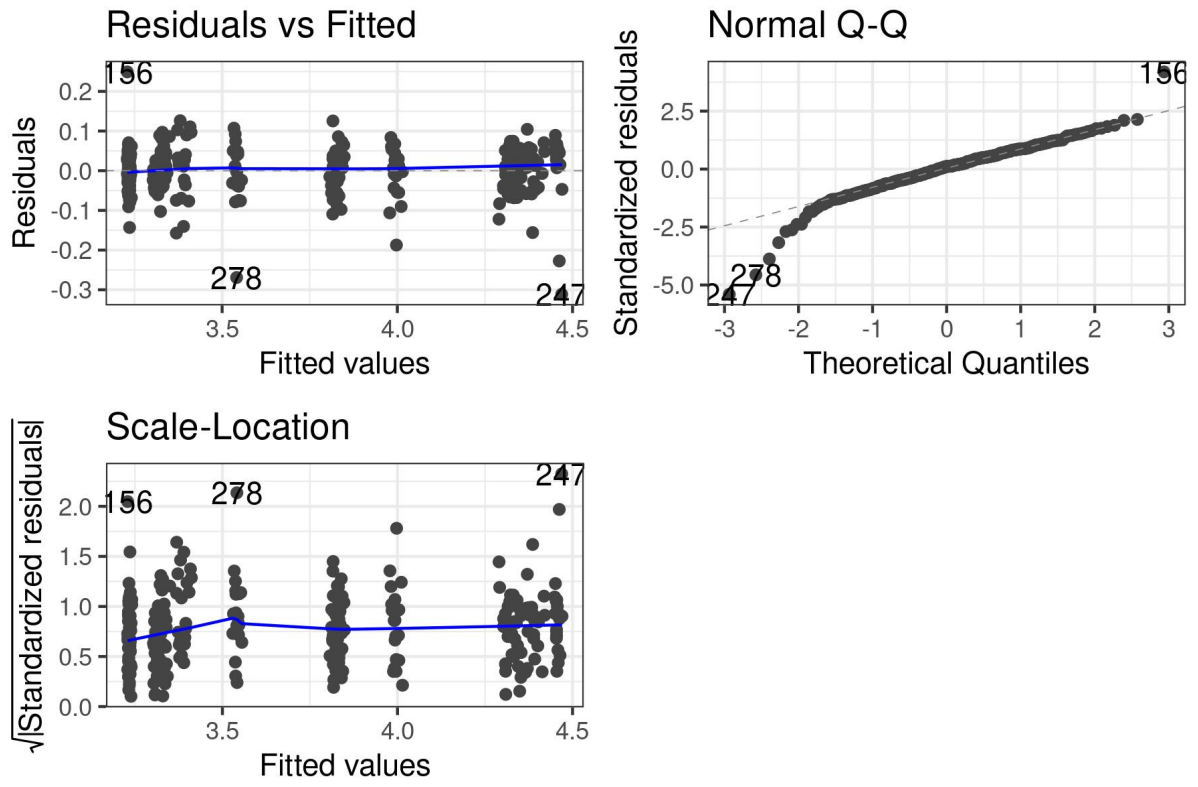

Source: MOBIS-Covid

Figure 20: Residual, Q-Q and scale-location plot for the RTLDT evening rush hour model.

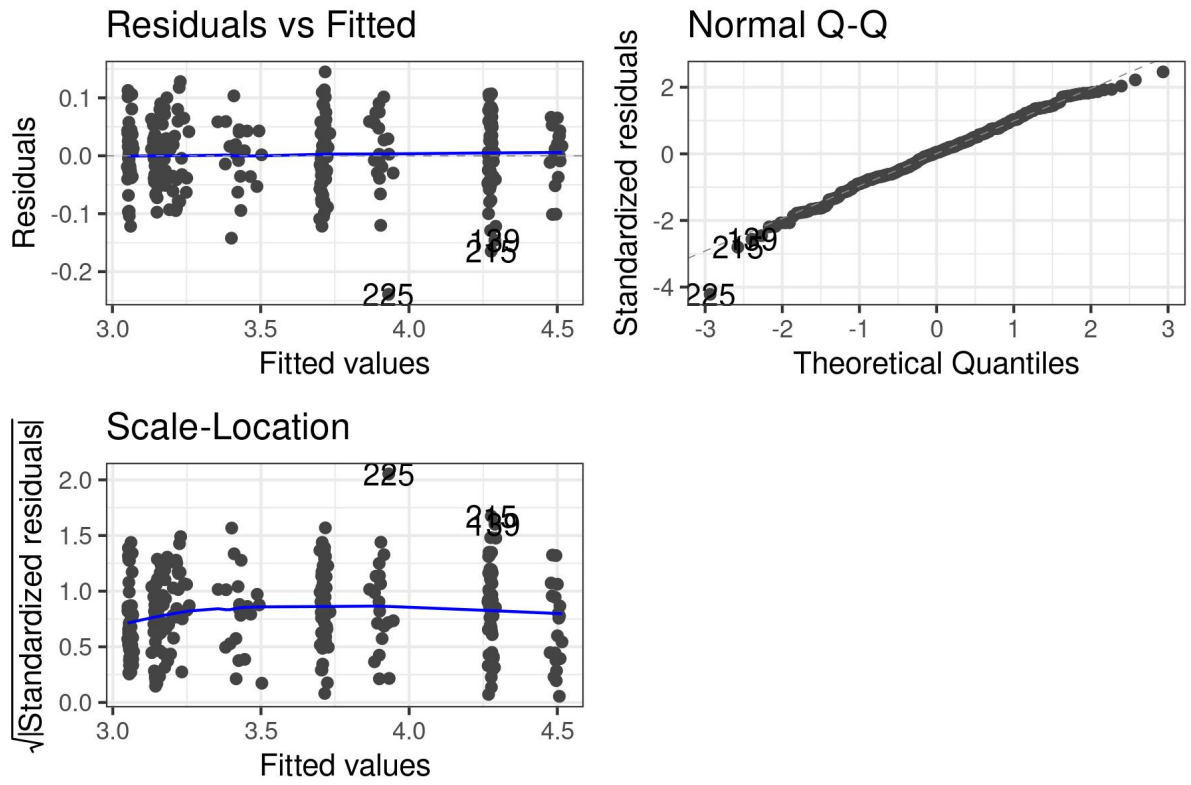

Source: MOBIS-Covid

Figure 21: Residual, Q-Q and scale-location plot for the Zürich (city) morning rush hour model.

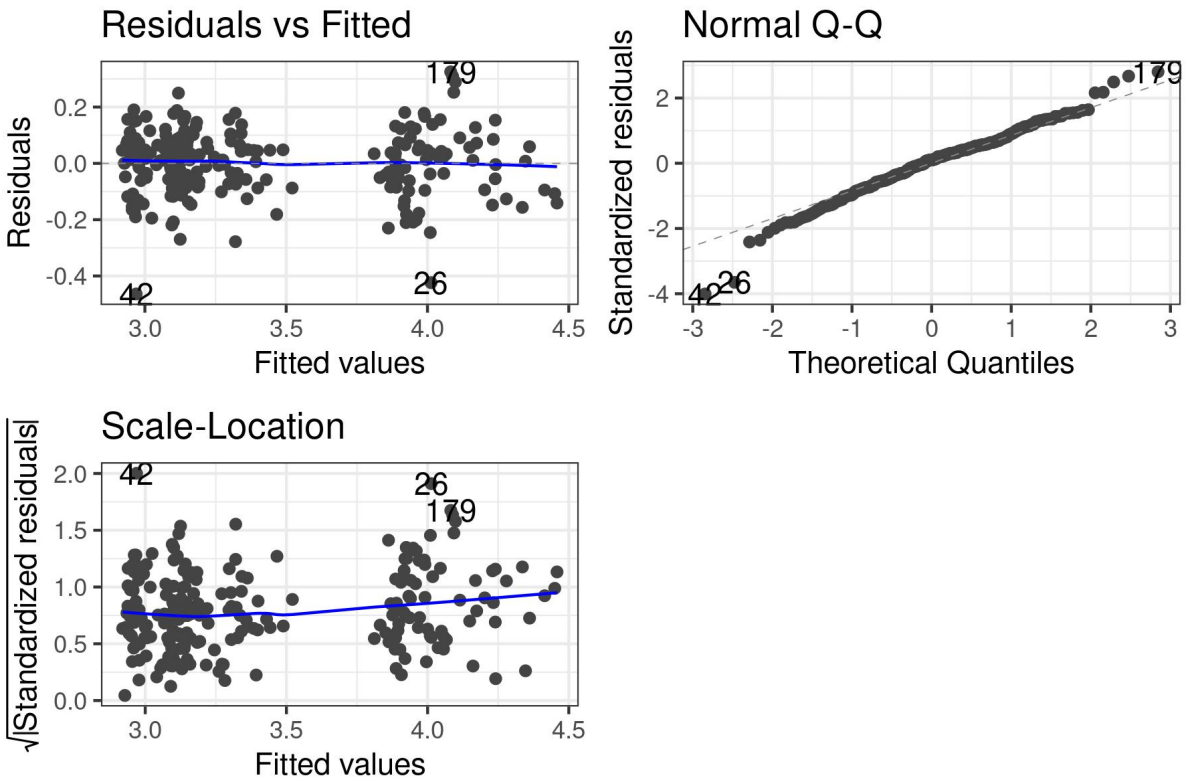

Source: MOBIS-Covid

Figure 22: Residual, Q-Q and scale-location plot for the Zürich (canton) morning rush hour model.

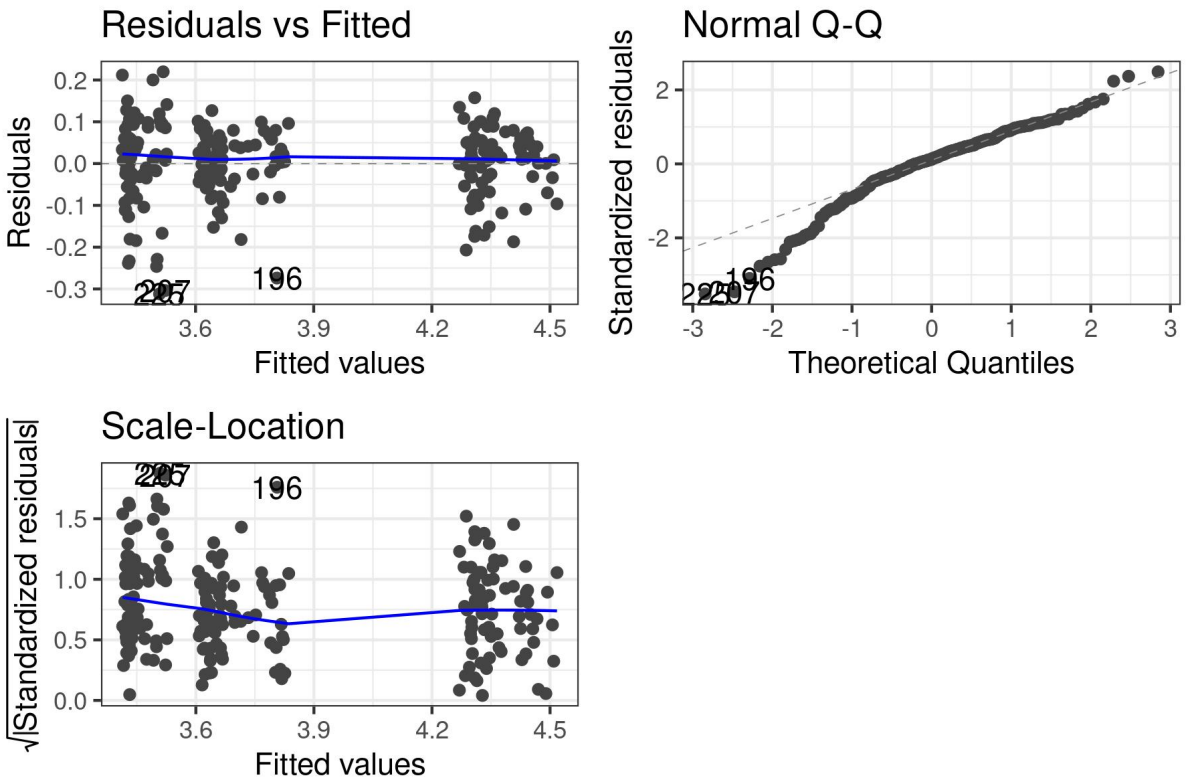

Source: MOBIS-Covid

Figure 23: Residual, Q-Q and scale-location plot for the Bern (city) morning rush hour model.

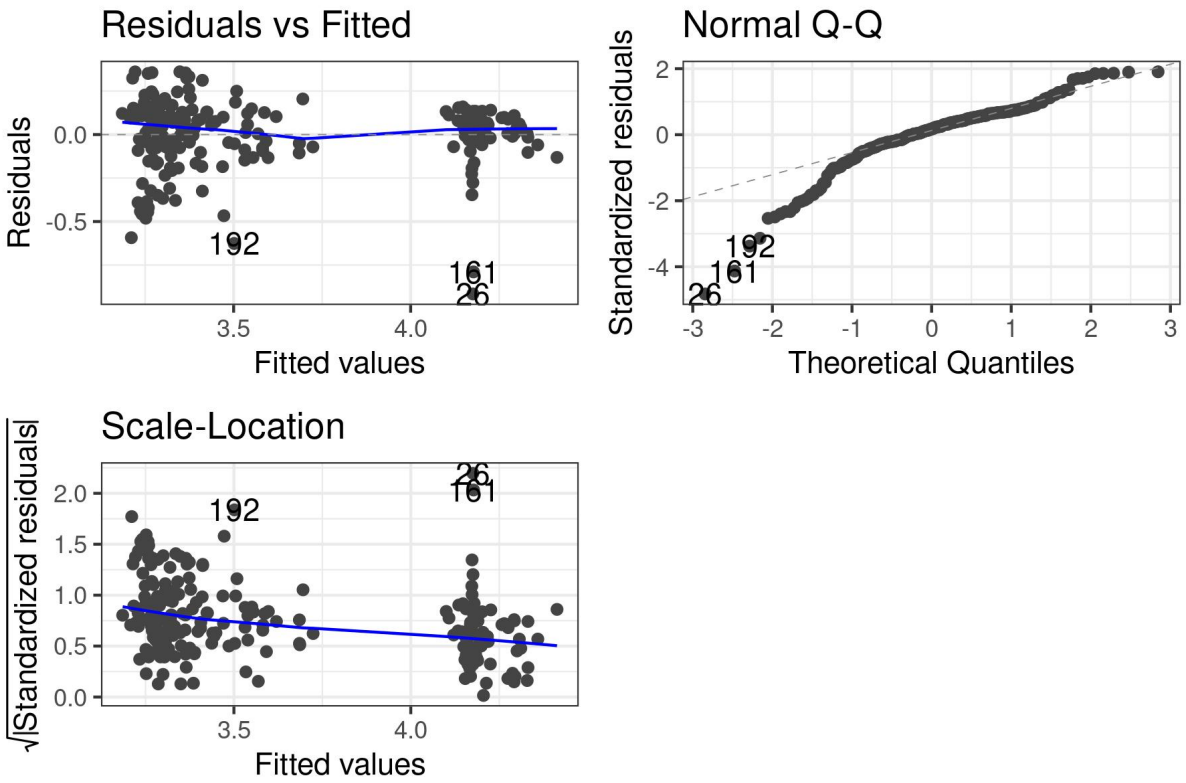

Source: MOBIS-Covid

Figure 24: Residual, Q-Q and scale-location plot for the Bern (canton) morning rush hour model.

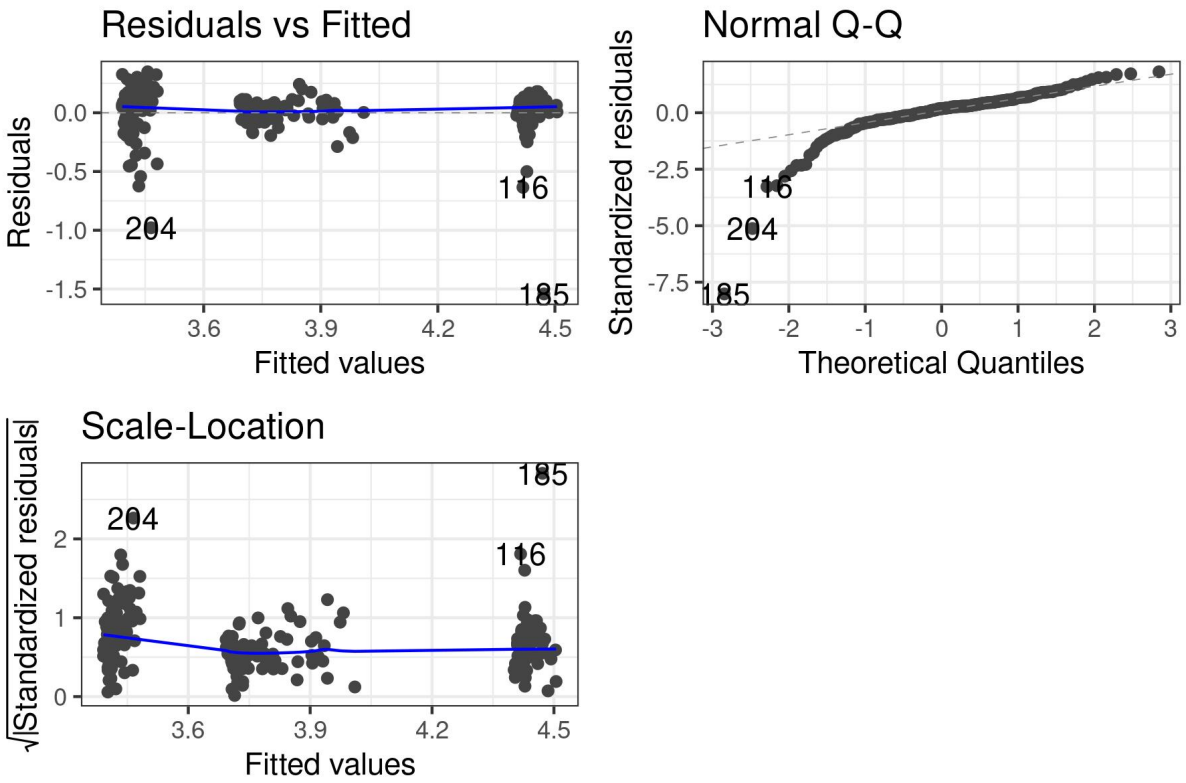

Source: MOBIS-Covid

Figure 25: Residual, Q-Q and scale-location plot for the Zürich (city) LD morning rush hour model.

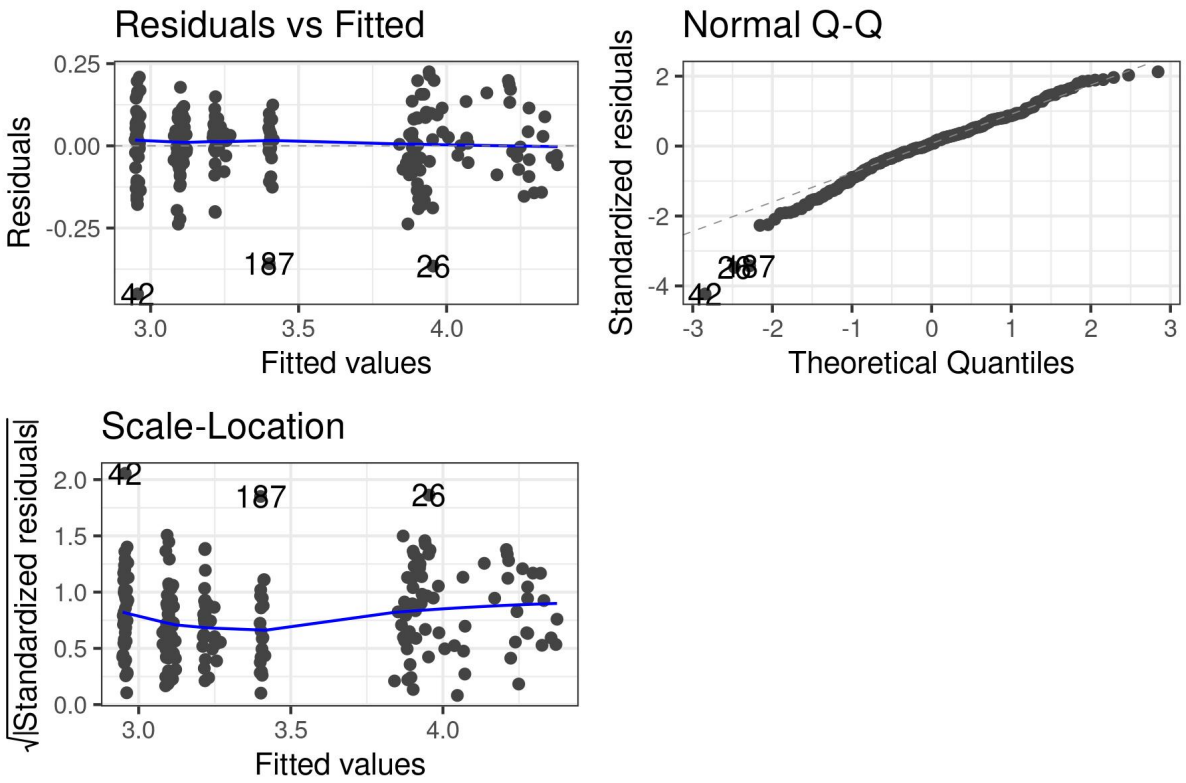

Source: MOBIS-Covid

Figure 26: Residual, Q-Q and scale-location plot for the Zürich (canton) LD morning rush hour model.

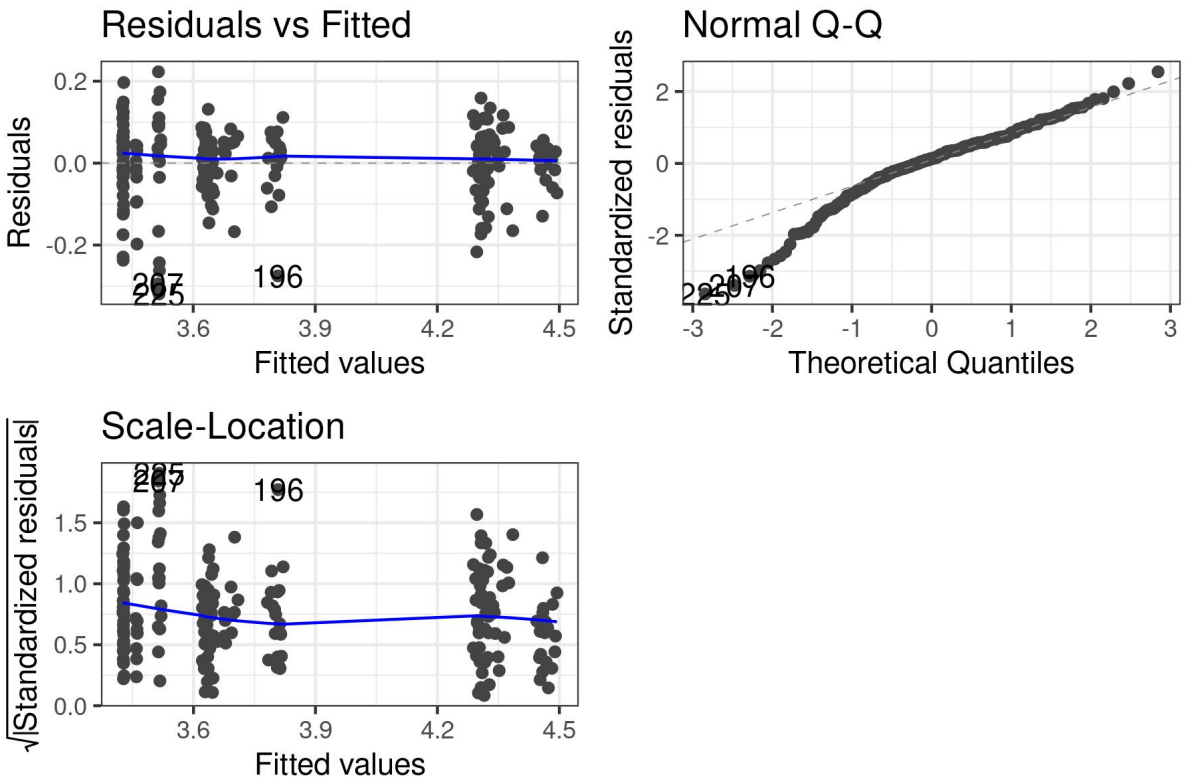

Source: MOBIS-Covid

Figure 27: Residual, Q-Q and scale-location plot for the Bern (city) LD morning rush hour model.

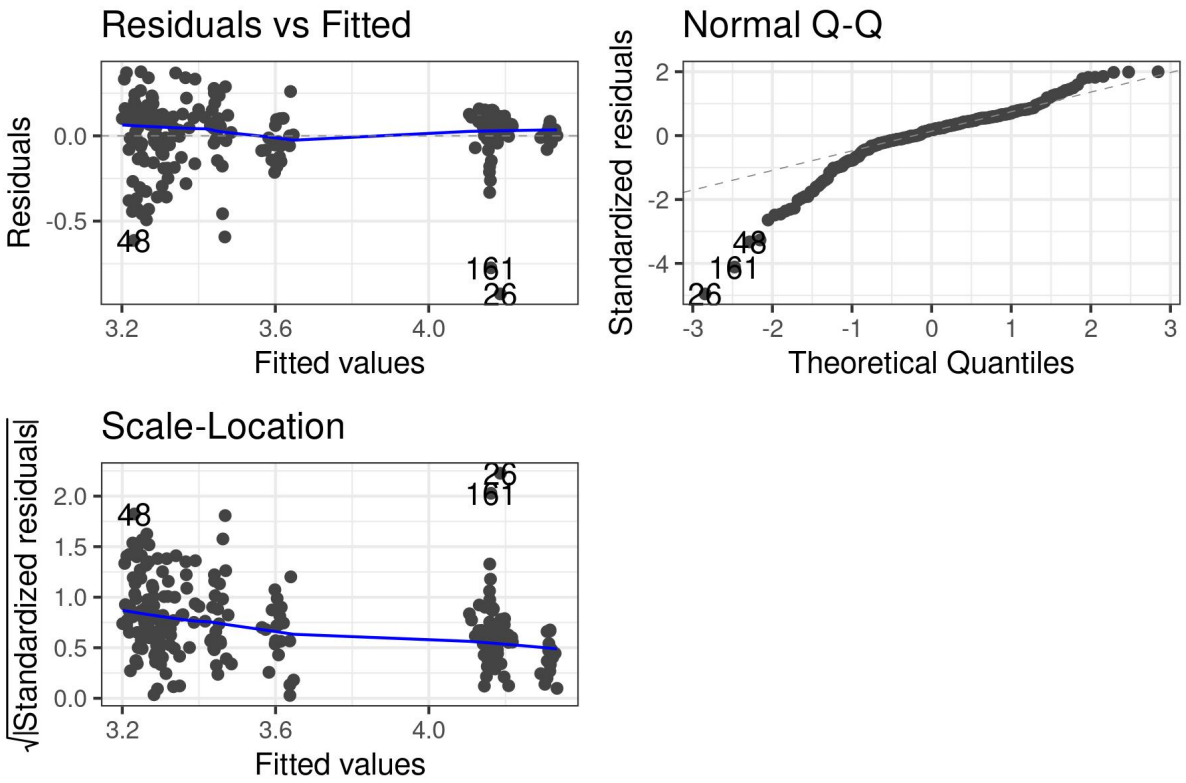

Source: MOBIS-Covid

Figure 28: Residual, Q-Q and scale-location plot for the Bern (canton) LD morning rush hour model.

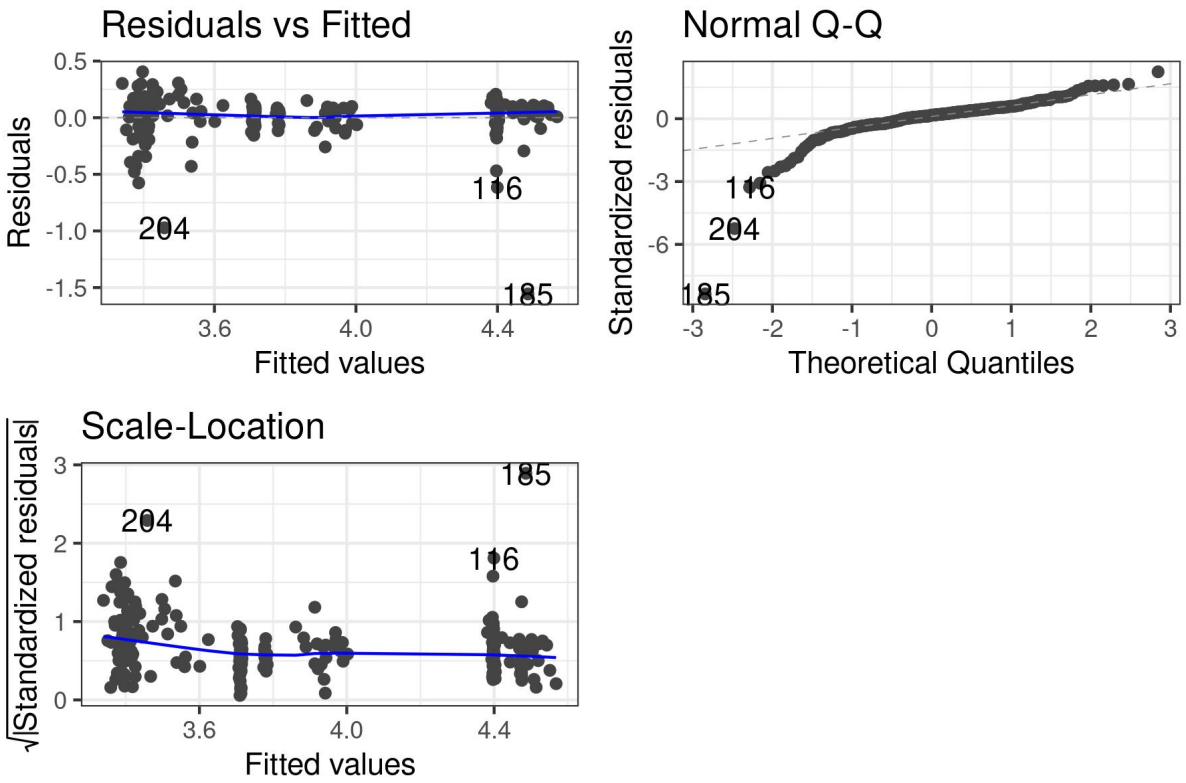

Source: MOBIS-Covid

Figure 29: Residual, Q-Q and scale-location plot for the Zürich (city) evening rush hour model.

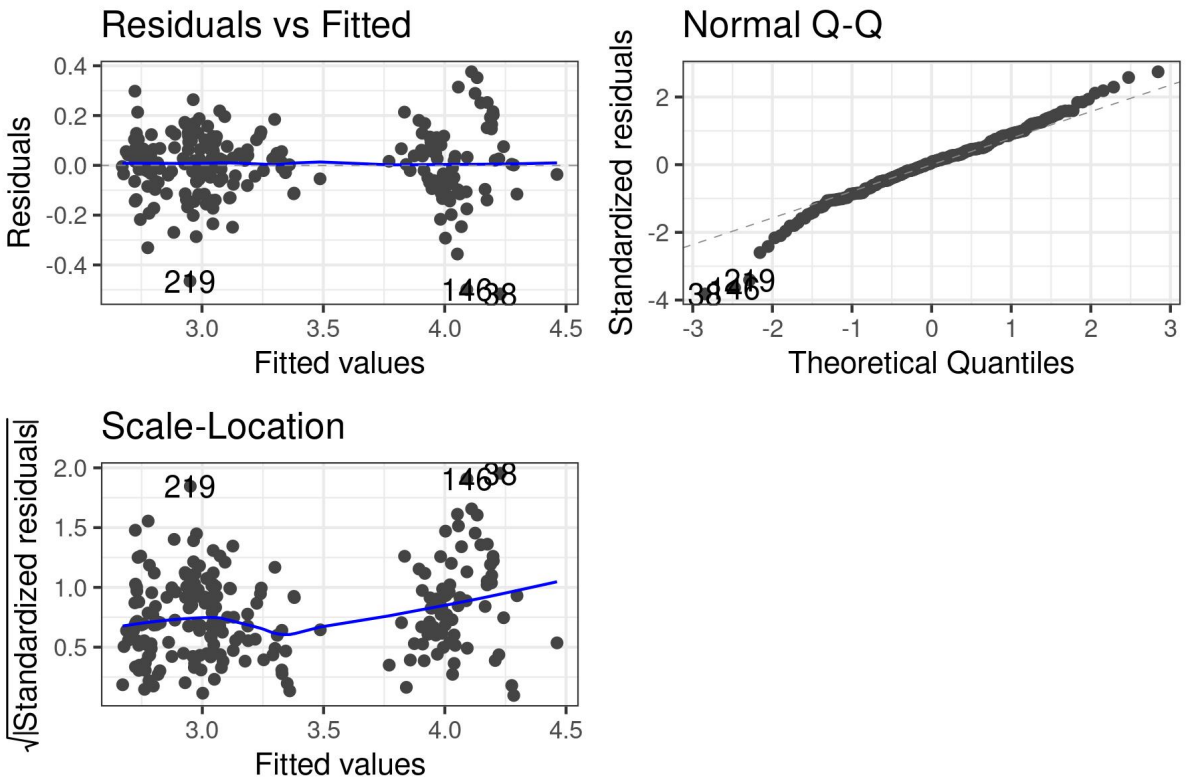

Source: MOBIS-Covid

Figure 30: Residual, Q-Q and scale-location plot for the Zürich (canton) evening rush hour model.

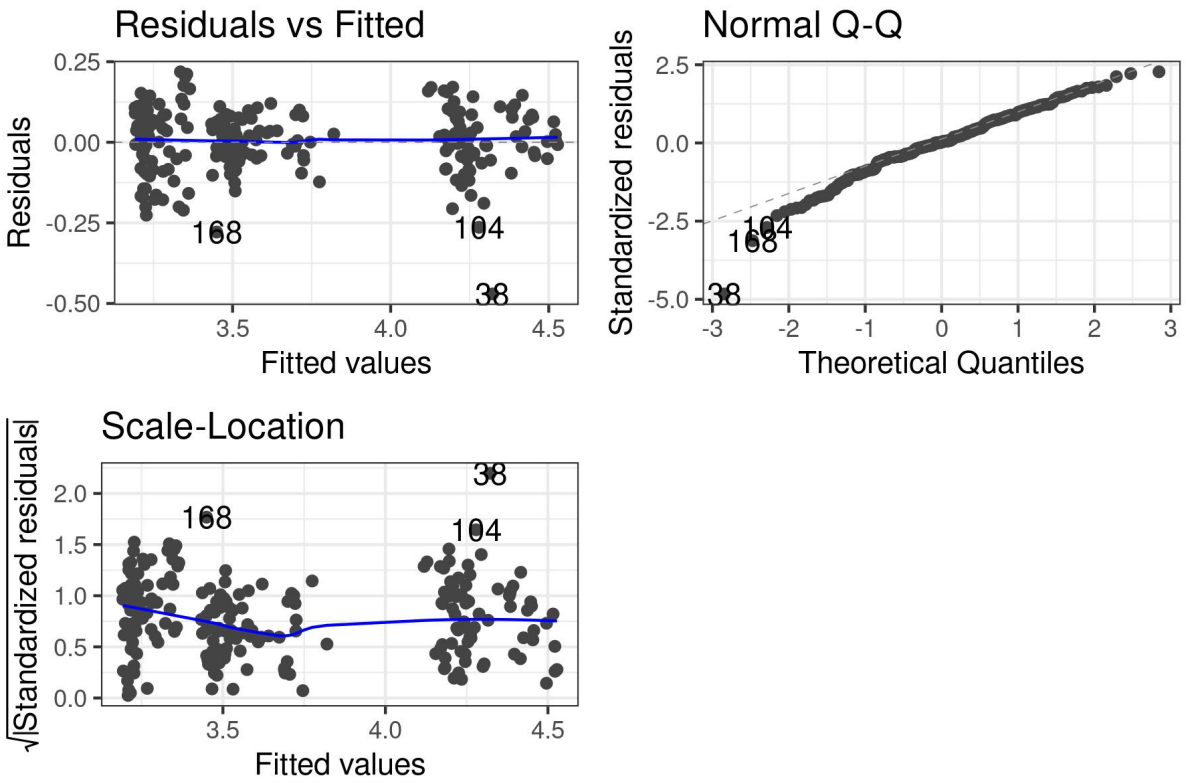

Source: MOBIS-Covid

Figure 31: Residual, Q-Q and scale-location plot for the Bern (city) evening rush hour model.

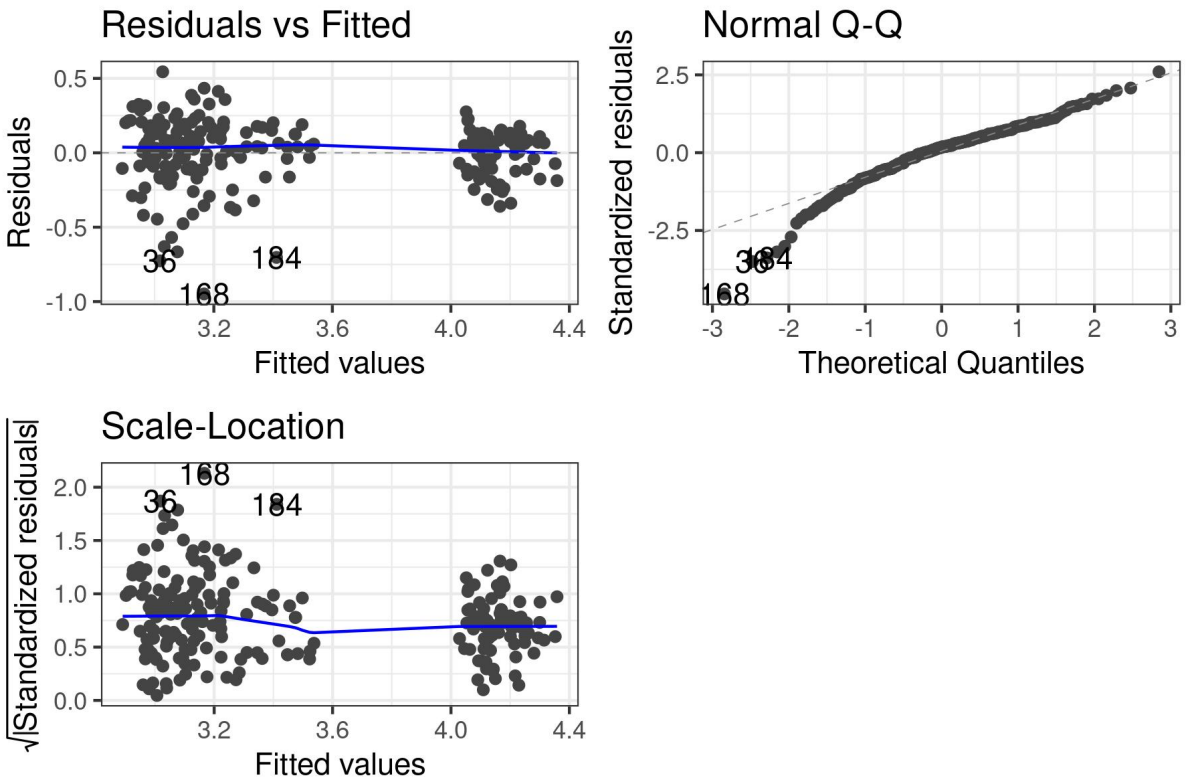

Source: MOBIS-Covid

Figure 32: Residual, Q-Q and scale-location plot for the Bern (canton) evening rush hour model.

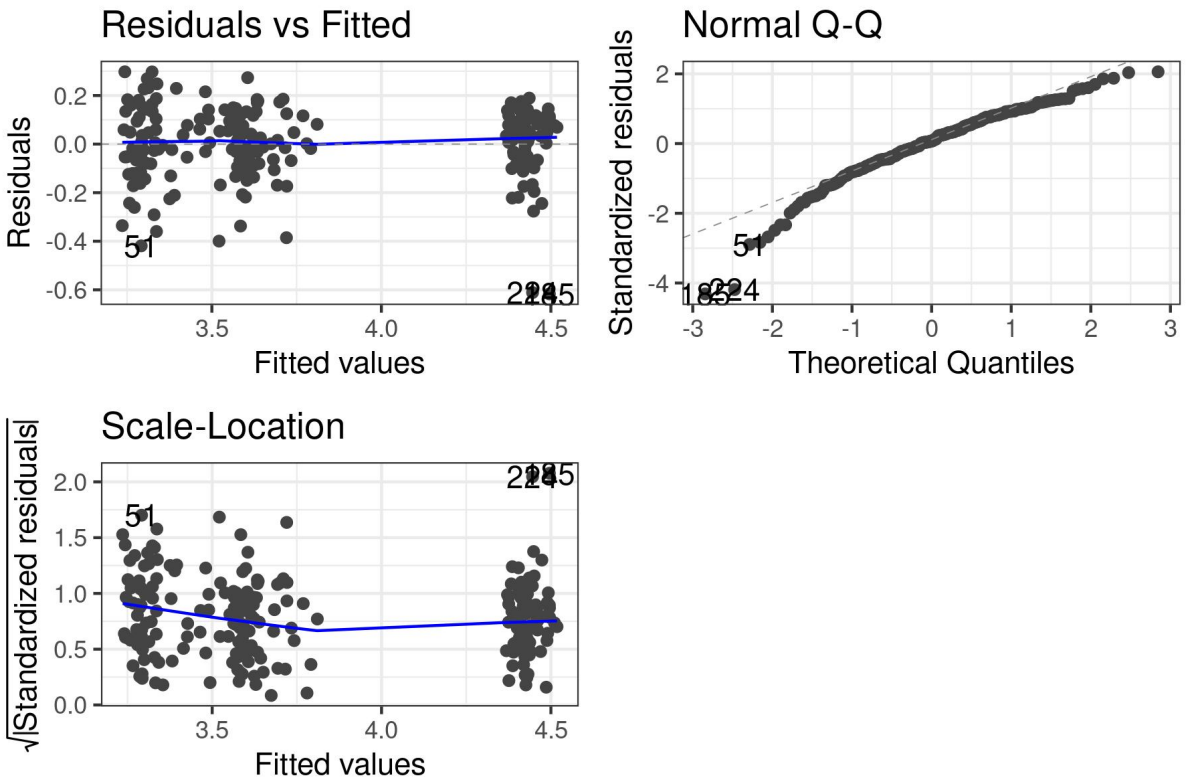

Source: MOBIS-Covid

Figure 33: Residual, Q-Q and scale-location plot for the Zürich (city) LD evening rush hour model.

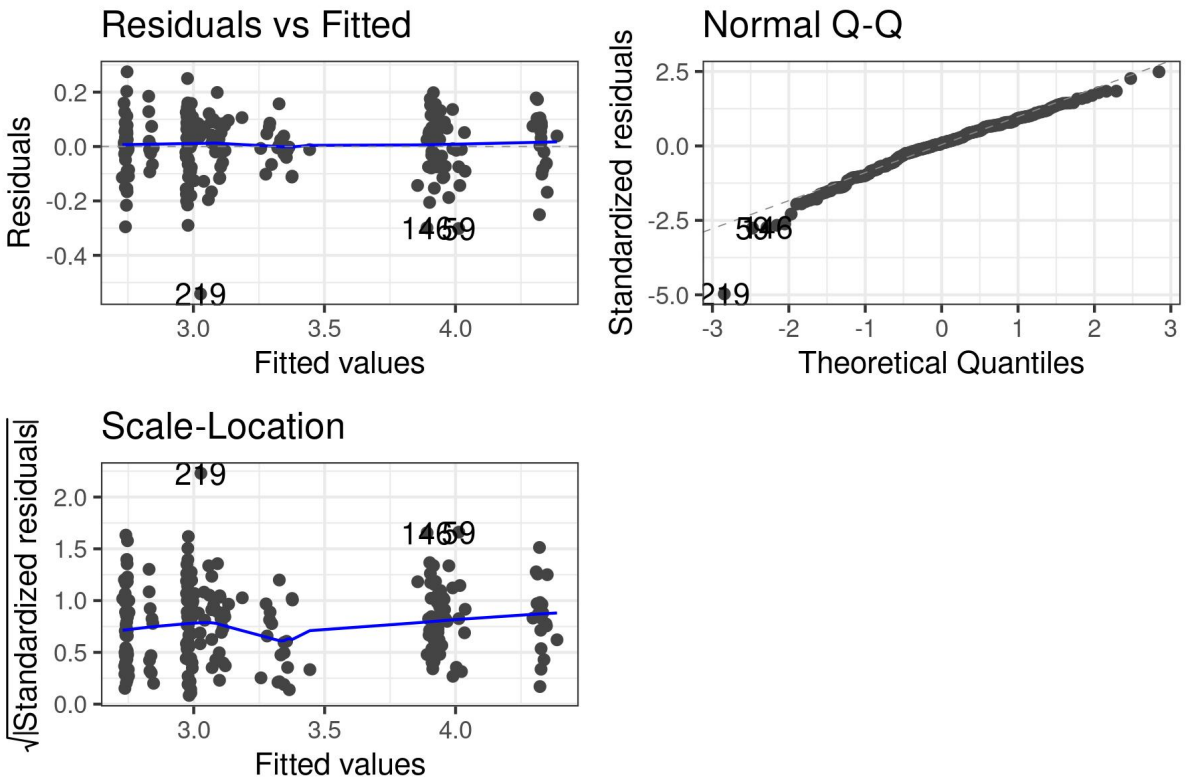

Source: MOBIS-Covid

Figure 34: Residual, Q-Q and scale-location plot for the Zürich (canton) LD evening rush hour model.

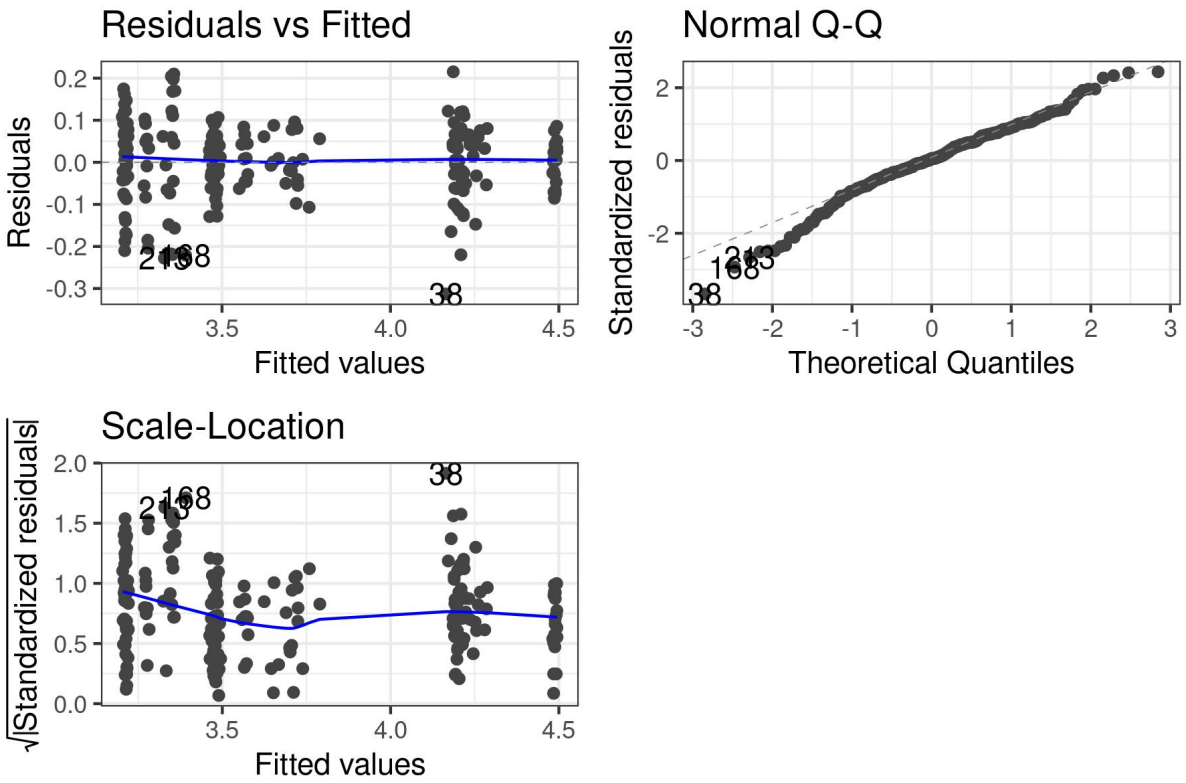

Source: MOBIS-Covid

Figure 35: Residual, Q-Q and scale-location plot for the Bern (city) LD evening rush hour model.

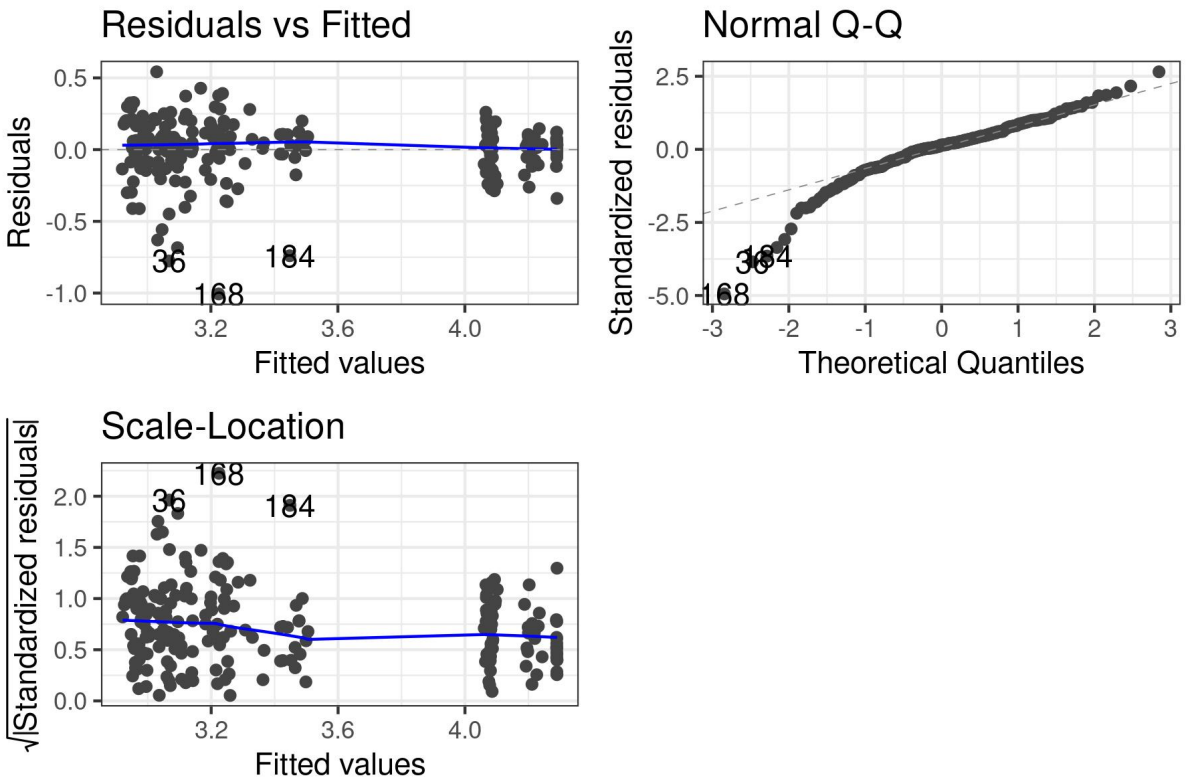

Source: MOBIS-Covid

Figure 36: Residual, Q-Q and scale-location plot for the Bern (canton) LD evening rush hour model.

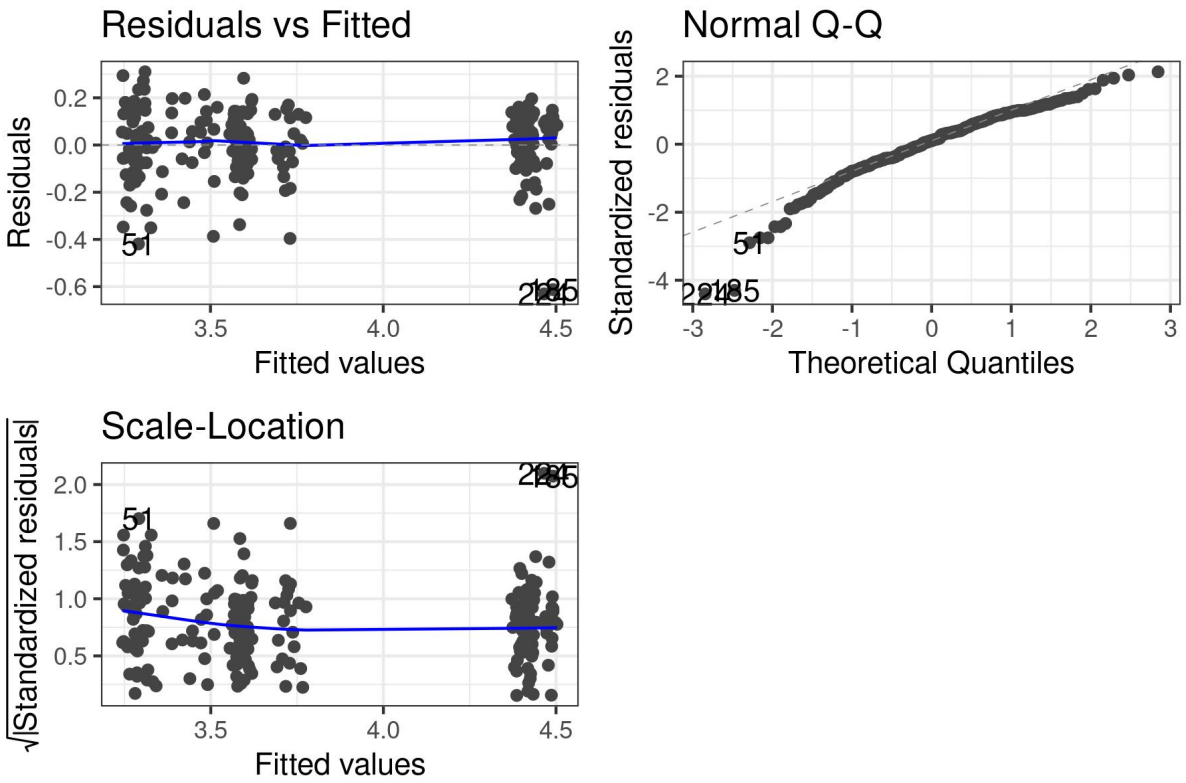

Source: MOBIS-Covid

Eidgenössische Technische Hochschule Zürich
Swiss Federal Institute of Technology Zurich

Declaration of originality

The signed declaration of originality is a component of every semester paper, Bachelor's thesis, Master's thesis and any other degree paper undertaken during the course of studies, including the respective electronic versions.

Lecturers may also require a declaration of originality for other written papers compiled for their courses.

I hereby confirm that I am the sole author of the written work here enclosed and that I have compiled it in my own words. Parts excepted are corrections of form and content by the supervisor.

Title of work (in block letters):

Modelling Spatial Average Speeds in Switzerland during the COVID-19 Lockdown

Authored by (in block letters):

For papers written by groups the names of all authors are required.

Name(s):	**First name(s):**
Zwyssig	Emanuel

With my signature I confirm that

- I have committed none of the forms of plagiarism described in the 'Citation etiquette' information sheet.
- I have documented all methods, data and processes truthfully.
- I have not manipulated any data.
- I have mentioned all persons who were significant facilitators of the work.

I am aware that the work may be screened electronically for plagiarism.

Place, date	**Signature(s)**
Cham, 23.6.2021	E. Zwyssig

For papers written by groups the names of all authors are required. Their signatures collectively guarantee the entire content of the written paper.